High resolution simulations reveal a large loss of Fennoscandian tundra due to climate change

Fredrik Lagergren[1], Robert G. Björk[2][3], Camilla Andersson[5], Danijel Belušić[5][6], Mats P. Björkman[2], Erik Kjellström[5], Petter Lind[5], David Lindstedt[5], Tinja Olenius[5], Håkan Pleijel[4], Gunhild Rosqvist[7] and Paul A. Miller[1]

[1]Department of Physical Geography and Ecosystem Science, Lund University, Lund, 223 62, Sweden

[2]Department of Earth Sciences, University of Gothenburg, Gothenburg, 405 30, Sweden

[3]Gothenburg Global Biodiversity Centre, Gothenburg, 405 30, Sweden

[4]Department of Biological & Environmental Sciences, University of Gothenburg, Gothenburg, 405 30, Sweden

[5]Swedish Meteorological and Hydrological Institute, Norrköping, 601 76, Sweden

[6]Department of Geophysics, Faculty of Science, University of Zagreb, Zagreb, 10 000, Croatia

[7]Department of Physical Geography, Stockholm University, Stockholm, 106 91, Sweden

Correspondence to: Fredrik Lagergren (Fredrik.Lagergren@nateko.lu.se)

Abstract. The Fennoscandian boreal and mountain regions harbour a wide range of vegetation types, from boreal forest to high alpine tundra and barren soils. The area is facing a rise in air temperature above the global average and changes in temperature and precipitation patterns. This is expected to alter the Fennoscandian vegetation composition and change the conditions for areal land-use such as forestry, tourism and reindeer husbandry. In this study we used a unique high-resolution (3 km) climate scenario with considerable warming resulting from strongly increasing carbon dioxide emissions to investigate how climate change can alter the vegetation composition, biodiversity and availability of suitable reindeer forage. Using a dynamical vegetation model, including a new implementation of potential reindeer grazing, resulted in simulated vegetation maps of unprecedented high resolution for such a long time period and spatial extent. The results were evaluated at the local scale using vegetation inventories and for the whole area against satellite-based vegetation maps. A deeper analysis of vegetation shifts related to statistics of threatened species was performed in six "hotspot" areas containing records of rare and threatened species. The simulations show dramatic shifts in the vegetation composition, accelerating at the end of the century. Alarmingly, the results suggest the southern mountain alpine region in Sweden will be completely covered by forests at the end of the 21st century, making preservation of many rare and threatened species impossible. In the northern alpine regions, most vegetation types will persist but shift to higher elevations with reduced areal extent, endangering vulnerable species. Simulated potential for reindeer grazing indicates latitudinal differences, where the current higher potentials in the south will diminish, while future potentials will increase in the north, especially for the summer grazing grounds. These combined results suggest significant shifts in vegetation composition over the present century for this scenario, with large implications for nature conservation, reindeer husbandry and forestry.

1 Introduction

High-latitude regions harbour vast areas of relatively intact ecosystems, holding species of great ecological, biological and societal significance. These northern ecosystems are predicted to be more vulnerable to climate change than most other terrestrial biomes (Hickler et al., 2012; IPCC, 2014). The observed temperature increase in Fennoscandia has been 2-3 degrees per degree of global average increase (Rantanen et al., 2022), with persistent trends in future predictions (Ono et al., 2022). This temperature increase has strongly affected northern ecosystems, resulting in changing vegetation patterns in the Arctic (Elmendorf et al., 2012; Pearson et al., 2013), an overall taller plant community (Bjorkman et al., 2018) and increases in biomass (Hudson and Henry, 2009). The occurrence and distribution of shrubs has also been observed to increase, both in high latitude and high-altitude regions, as a result of the warmer climate (Elmendorf et al., 2012; Myers-Smith et al., 2011; Sturm et al., 2001). The distance species have to migrate to keep up with climate change is, however, shorter in alpine and Oroarctic regions than in flat boreal and Arctic landscapes (Feeley et al., 2011). As the boreal forest covers a wide area, its species composition and ability to provide ecosystem services could undergo large shifts, e.g. as a response to different disturbance patterns and hydrology changes (Venäläinen et al., 2020), even if its geographical extent is not changed. Consequences of future shifts in areal extent of vegetation zones, which may not be proportional to their current distributions, include reduced space of many habitats (Pauli and Halloy, 2019) and increased pressure on many species (Kuuluvainen and Gauthier, 2018).

The Fennoscandian boreal and Oroarctic region is located between 58 and 71 °N, spanning altitudes from sea level to 2469 m a.s.l. (Galdhöpiggen, Norway), and is characterised by continental to sub-oceanic climate (Oksanen and Virtanen, 1995). Boreal forest dominates from the coast towards the mountains up to latitude 68-69 °N. Above the boreal forest there is a zone of mountain birch forest which normally has a vertical distribution of ca 200 m. The tree-line, formed by mountain birch, is in Sweden at an altitude of more than 1100 m in the south and decreases with latitude to 600 m in the north (Kullman, 2016). Above the tree line follows tundra with decreasing levels of vegetation height and coverage (from shrub- to barren tundra) and finally bare rocks and snowfields.

The herding of semi-domesticated reindeer is important in shaping this landscape, a practice which utilises the land from the coastal areas and the boreal forest in winter up to the tundra in summer (Käyhkö and Horstkotte, 2017). Reindeer grazing directly affects the vegetation composition and diversity, both in the mountains (Olofsson et al., 2001; Sundqvist et al., 2019; Vowles et al., 2017) and forested regions (Kumpula et al., 2014). In summer, reindeer have a mixed diet of shrub leaves, forbs, herbs, sedges, grass, and fungal fruit bodies, and reindeer forage has been shown to reduce deciduous shrub expansion (e.g. Olofsson et al., 2001; Olofsson et al., 2009; Sundqvist et al., 2019; Vowles et al., 2017). In winter, reindeer mainly eat ground- and tree-lichens, which decreases ground-lichen cover (Kumpula et al., 2014). However, reindeer husbandry is currently experiencing increased pressure from human activities, such as forestry practices and tourism (Fohringer et al., 2021; Kumpula et al., 2014; Sandström et al., 2016), affecting 85% of the herding area (Stoessel et al., 2022). In addition, there are implications resulting from climate change, such as difficult snow conditions making winter forage hard (Rasmus et al., 2022; Rosqvist et al., 2021) and hot dry summers increasing heat stress (Käyhkö and Horstkotte, 2017). Climate change

75   is increasing the pressure on both ecosystems and societies in these areas, a pressure that will increase in coming

76   decades (Constable et al., 2022).

77

78   Projections of future impacts of climate change in high latitude ecosystems can be made upon the implementation

79   of understanding arising from empirical studies (e.g. Bjorkman et al., 2020; Myers-Smith et al., 2011) and remote

80   sensing (e.g. Callaghan et al., 2022), into models such as dynamical vegetation models (DVMs) using climate

81   model data as input. The typical cell size of a regional climate model (on the order of 10-50 km) often contains

82   land surface types ranging from forest to bare rock or glaciers in mountainous areas. This information does not

83   capture all local variation, especially in areas of complex terrain where altitudinal differences can be strongly

84   underestimated. Also, while representing most meteorological processes some are only crudely implemented at

85   such relatively coarse resolution in modelling studies (Lind et al., 2020). In recent years, DVMs have been adapted

86   to the boreal and Arctic regions (Miller and Smith, 2012; Wolf et al., 2008; Yu et al., 2017), and very highly

87   resolved climate data (e.g. 50×50 m) have been used only at a local scale in sub-arctic Scandinavia (Gustafson

88   et al., 2021; Tang et al., 2015). So far, however, no high-resolution study of environmental change and its impact

89   on vegetation covering the entire Fennoscandian boreal and Oroarctic region has been made.

90

91   Recently the first ever km-scale climate model projections were completed for the entire Fennoscandian region

92   (Lind et al., 2020; Lind et al., 2022). Results from such km-scale simulations offer an unprecedented insight into

93   weather and climate processes at high resolution, which is particularly important in complex terrain. Thus, we

94   here use this unique km-scale climate model projections for the high-emission RCP8.5 scenario (Lind et al., 2022)

95   and a state-of-the-art DVM; LPJ-GUESS (Smith et al., 2001; Smith et al., 2014) to investigate the vegetation

96   response to climate and environmental change in the Fennoscandian boreal and mountain regions. The results are

97   validated against satellite products and field data gathered in the study region. Furthermore, we use consistent,

98   high-resolution climate and nitrogen deposition scenarios to evaluate potential future vegetation changes in the

99   region, with a special emphasis on reindeer food supply and vegetation trends in "hotspot" areas with high biodi-

100 versity and conservation values.

101

2 Material and methods

2.1 Study area

104 The study was restricted to the Fennoscandian mountain range and the adjacent boreal areas used for reindeer

105 herding (Figure 1), with a focus on ecosystems in Sweden. For a more detailed assessment of simulated changes,

106 six "hotspot" areas (90×90 km) in the larger domain were selected to represent different vegetation zones with a

107 high species richness and large conservation values, from the boreal forest to the high alpine tundra and covering

108 the entire Swedish mountain range (Table 1, Figure 1, Figure S1):
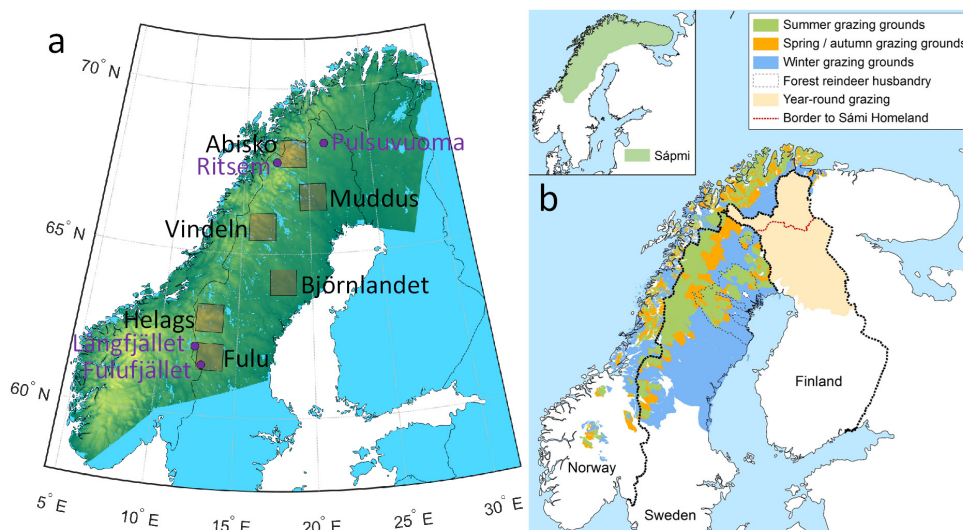
109

110 **Figure 1.** a) The study area (shown as altitude from sea level (dark green) to 2000 m a.s.l. (yellow), the six focus "hotspot"

111 areas (shaded squares and black text, see Figure S1 for detailed maps) and the four grazing exclosure sites (purple dots and

112 text). b) Map of grazing areas used for the semi-domesticated reindeer during different seasons in Norway, Sweden and Finland

113 (from Käyhkö and Horstkotte (2017), used with permission).

114

115 **Table 1.** Description of the six "hotspots". Maps of the areas are shown in Figure S1.

Name	Coordinates	Type	Protected area	Description
Abisko	68° 01' N, 18° 46' E	Mountain	Abisko National Park, established 1909	Including the highest mountains (2097 m) in Sweden
Vindeln	65° 49' N, 16° 29' E	Mountain	Vindelfjällen Nature Reserve, established 1974	Including mountains reaching 1768 m
Helags	62° 58' N, 13° 06' E	Mountain	Vålådalen Nature Reserve, established 1988	Including the mountain Helags (1797 m)
Fulu	61° 47' N, 13° 17' E	Mountain	Fulufjället National Park, established 1973	At the southernmost part of the Scandes mountains (1196 m, Sömlinghågna) in Sweden
Muddus	66° 43' N, 20° 17' E	Forest	Muddus National Park, established 1942	Mostly boreal forest with extensive wetlands
Björnlandet	64° 07' N, 18° 01' E	Forest	Björnlandet National Park, established 1991	Boreal forest with some wetlands

116

2.2 Dynamical vegetation and ecosystem model

118 The dynamical vegetation and ecosystem model LPJ-GUESS (v4.1, Gustafson et al., 2021; Smith et al., 2001;

119 Smith et al., 2014) was used to simulate vegetation change in the region. The model simulates the development

120 of cohorts belonging to different plant functional types (PFTs) when competing for light, nitrogen and water in

121 replicate patches representing an area of ca 1000 m^2 (here set to 15 patches per simulated climate gridcell). The

122 model includes detailed process descriptions related to the cycling of water (e.g. transpiration, evaporation, and

123   snow and soil water dynamics), carbon (e.g. photosynthesis, respiration, fire, and allocation of biomass), and
124   nitrogen (e.g. nitrification and restriction of photosynthesis), and is driven by temperature, radiation, relative hu-
125   midity, wind speed, CO_2 concentration, and nitrogen deposition data. The PFTs are described by parameters re-
126   lated to growth form (tree, shrub or herbaceous), allocation, allometry, phenology, life history, shade tolerance
127   and response to environmental and bioclimatic conditions. Patch destroying disturbances representing e.g. devas-
128   tating pests or wind storms, occur randomly in each patch (return time set to 150 years in the presented simula-
129   tions). A simulation starts after a spin-up period (set to 600 years) over which a detrended dataset comprising the
130   first 30 years of historical climate data are repeated to get the vegetation in balance with the climate.

131

132   2.2.1 Plant functional types

133   In the present study, an expanded set of PFTs were used for mineral soils, including high-latitude PFTs such as
134   shrubs (Table 2).

135

136   **Table 2.** Plant functional types in the LPJ-Guess simulations. The last six PFTs were used for the wetland simulation and the
137   rest for mineral soils.

PFT	Long name	Typical represented species
BNE	Boreal needle-leaved evergreen tree, shade tolerant	*Picea abies*
BINE	Boreal needle-leaved evergreen tree, shade intolerant	*Pinus sylvestris*
IBS	Shade-intolerant broadleaved summergreen tree	*Betula pubescens* ssp. *tortuosa*
TeBS	Shade-tolerant temperate broadleaved summergreen tree	*Fagus, Quercus, Fraxinus* spp
C3G	Cool (C3) grass	
HSE	Tall shrub (up to 2m), evergreen	*Juniperus communis*
HSS	Tall shrub (up to 2m), summergreen	*Alnus* spp., *Salix* spp., *Betula nana*
LSE	Low shrub (up to 0.5m), evergreen	*Vaccinium vitis-idaea, Empetrum* spp.
LSS	Low shrub (up to 0.5m), summergreen	*Vaccinium myrtillus*, small *Salix* spp.
GRT	Graminoid and forb tundra	Grass, sedge and forb tundra species
EPDS	Evergreen prostrate (up to 0.2m) dwarf shrubs	*Vaccinium oxycoccos, Cassiope* spp*., Dryas octopetala, Saxifraga* spp.
SPDS	Summergreen prostrate (up to 0.2m) dwarf shrubs	Dwarf *Salix* spp., *Arctostaphylos alpinus*
CLM	Cushion forb, lichen and moss tundra	*Saxifragaceae, Caryo-phyllaceae, Draba* spp., lichens, mosses
pLSE	Peatland low shrub, evergreen	*Vaccinium vitis-idaea, Cassiope* spp.
pLSS	Peatland low shrub, summergreen	*Vaccinium myrtillus, V. uliginosum, Salix hastata, S. glauca*
pCLM	Peatland cushion forb, lichen and moss tundra	*Saxifragaceae, Caryophyllaceae, Papaver* spp*., Draba* spp., lichens, mosses
WetGRS	Cool, flood-tolerant (C3) grass	*Carex* spp., *Eriophorum* spp., *Juncus* spp., *Typha* spp.
pmoss	Peatland moss	
C3G_wet	Peatland cool (C3) grass	

138

139   For fractions of land classified as peatland, we use a version of the model with peatland integration (Wania et al.,
140   2009a, b), which include a wetland hydrology module and wetland PFTs (Miller and Smith, 2012; Wolf et al.,
141   2008; Zhang et al., 2013). The fractions of mineral soil and wetland were prescribed and constant over the simu-
142   lation period based on the PEATMAP product at a 0.125° resolution (Xu et al., 2018). Weighted averages of
143   model results were calculated based on these fractions. Test runs showed underestimation in the spatial extent of
144   the shade-intolerant broadleaved summergreen tree (IBS) PFT, which represents the mountain birch (*Betula pu-*
145   *bescens* ssp. *tortuosa*) forest that normally forms the tree-line in Fennoscandia. A fine-tuning of some of the
146   model's parameters was therefore done to get a better match against distribution maps from observations (Table
147   S2).
148

149   **2.2.2 Reindeer grazing, browsing and trampling**

150   To simulate the effect of reindeer grazing, browsing and trampling, a new module was added to the model. Graz-
151   ing/browsing was simulated by removing a fraction of leaf biomass. Trampling was simulated by killing a fraction
152   of the individuals in a cohort, or, in the case of herbaceous PFTs, a fraction of total biomass. The grazing/browsing
153   and trampling level was based on a constant intensity of herbivory. For a specific PFT, the grazing/browsing was
154   determined by a preference value obtained from extensive observations of the feeding preferences of semi-do-
155   mesticated reindeer in Canada (Denryter et al., 2017) and if the cohort's canopy height was within reach of rein-
156   deer. The sensitivity to trampling was based on the vegetation response in an artificial trampling experiment
157   (Egelkraut et al., 2020). All the consumed carbon in the leaves was treated as harvested but only a fraction of the
158   leaf nitrogen. The other fraction of the consumed N was added to the cohort's leaf N pool, which reflects the
159   assumption that N leaving the herbivore as urine is directly taken up by the plants (Barthelemy et al., 2018). A
160   detailed description of the module and its parameter values is given in S3. From this module, the resulting output
161   of consumed C biomass was used as an indicator of potential reindeer food consumption. In the presented simu-
162   lations, the simulated grazing, browsing and trampling in a patch was set to have a return time of 3 years (see S3
163   for motivation), a grazing intensity of 0.1 (fraction yr^{-1}), a max height of 2.5 m and that 35% of browsed nitrogen
164   (Ferraro et al., 2022; Mcewan and Whitehead, 1970) was removed to the harvest pool.
165

166   **2.3 Model input data: climate**

167   The regional climate modelling system HCLIM38 (Belušić et al., 2020) was used for downscaling the RCP8.5
168   scenario simulation from the global climate model EC-Earth (Hazeleger et al., 2010; Hazeleger et al., 2012). The
169   climate scenario was first downscaled to 12 km with HCLIM38-ALADIN for the period 1985-2100 and then
170   further to 3 km with HCLIM38-AROME for the periods 1985-2005, 2040-2060 and 2080-2100 (Lind et al., 2020;
171   Lind et al., 2022).
172

173   The years 1985 in the ALADIN 12 km data and 1985, 2040 and 2080 in the AROME 3 km data were spin-up
174   years. To test the robustness of the results, all climate variables used by the vegetation model were also compiled
175   (see below) without using the HCLIM spin-up years and tested on a sub-set of 200 random gridcells. As there

176 were no significant differences in the results we present results based on climate data including the HCLIM spin-
177 up years.

178

179 For filling the periods when only ALADIN data were available, datasets were first made such that the four
180 AROME gridcells coinciding with a certain ALADIN gridcell were filled with data from that ALADIN gridcell
181 (ALAatARO, 1985-2100). The periods with missing 3-km AROME data were filled with the ALAatARO data
182 using two methods. For precipitation, global radiation, relative humidity, and wind speed, linear regressions
183 through origin for the overlapping periods between AROME data and the ALAatARO data were used. The rela-
184 tions were fitted separately by month and, specifically, data from 1985-2005 and 2040-60 were used to establish
185 the relationships for the 2006-2039 period, and 2040-2060 and 2080-2100 for the 2061-2079 period. The relation-
186 ships were then used to get 3-km data for the missing periods from ALAatARO data.

187

188 For daily, minimum and maximum temperatures a non-parametric empirical quantile mapping "QUANT" bias
189 correction method (e.g. Osuch et al., 2017) was applied by month using daily temperature data for 21-year periods.
190 Two reference periods were used with observed 1 × 1 km data from Nordic Gridded Climate Dataset (NGCD,
191 https://surfobs.climate.copernicus.eu/dataaccess/access_ngcd.php) that were aggregated to the AROME grid,
192 1985-2005 (used for AROME grid data) and 1998-2018 (used for ALAatARO grid data). In the quantile mapping,
193 intervals of 1% were applied and a smoothing was done using a running mean over 5 intervals. Modelled and
194 matching observed values were linearly interpolated between the intervals. For consistency, all calculations of
195 quantiles were done for 21-year periods, resulting in an overlapping period (1998-2005) for which the AROME
196 data were used. For the future, the difference between observed and scenario quantiles during the reference period
197 was added to the matching quantile of future 21-year periods. The future periods were 2040-2060 and 2080-2100
198 for the AROME data and 2019-2039 and 2060-2080 (2060 and 2080 not used) for the ALAatARO data.

199

200 The RCP8.5 scenario used was the first dataset produced at this high resolution for the entire region. It is a scenario
201 with strongly increasing emissions of greenhouse gases, but the projection up to the mid-century is similar to
202 lower emission scenarios (Meinshausen et al., 2011). In the resultant daily air temperature data, the climate-change
203 signal was a 1.0-2.3 K increase in mean annual temperature from the 1991-2020 to the 2031-2060 30-year periods,
204 and a 2.5-5.2 K increase from 1991-2020 to 2071-2100 (Figure S4a-b). For annual precipitation the relative change
205 was -2.3 – 23.1% to 2031-2060 and -0.9 – 50.1% to 2071-2100 (Figure S4c-d).

206

207 **2.4 Model input data: soil texture, atmospheric nitrogen deposition and CO_2**

208 Soil texture data (clay and sand fraction) at 3 km resolution were taken from SURFEX (Masson et al., 2013), the
209 land surface model of AROME, ensuring consistency with LPJ-GUESS. These data originate from FAO soil
210 texture data at 5 arc seconds (10 km) resolution (https://data.apps.fao.org/map/catalog/static/search?key-
211 word=DSMW) that had been interpolated to 3 km resolution.

212

213 Nitrogen deposition at monthly temporal resolution was used as input to LPJ-GUESS. The input was based on
214 two model simulations (MATCH-BIODIV and MATCH-ECLAIRE) with the Multi-scale Atmospheric Transport

215 and Chemistry (MATCH, Andersson et al., 2015; Andersson et al., 2007; Robertson et al., 1999) model. MATCH-
216 BIODIV (Andersson et al., Manuscript; Eichler et al., 2023) was forced by the climate simulation ALADIN at 12
217 km, and anthropogenic air pollution emissions from ECLIPSE V6b (Höglund-Isaksson et al., 2020). This data set
218 (https://previous.iiasa.ac.at/web/home/research/researchPrograms/air/ECLIPSEv6b.html, accessed Feb 2020) has
219 a resolution of 12 km and covers the period 1987-2051. MATCH-ECLAIRE (Engardt et al., 2017) was constructed
220 at 50 km resolution for 1900-2050, based on current climate and varying anthropogenic air pollutant emissions
221 ECLIPSE V4a and Lamarque et al. (2010).

222

223 MATCH-ECLAIRE was used to obtain 12 km resolution nitrogen deposition fields for the time period 1900-
224 1986. This was done by establishing a linear relationship through zero for the overlapping period for each
225 MATCH-BIODIV and MATCH-ECLAIRE gridcell and subsequently applying it to downscale the 50 km data
226 for the 1900-1986 period. After 2051, the 0.5° resolution Lamarque et al. (2011) dataset was used, which is stand-
227 ard for LPJ-GUESS.

228

229 The future trend in nitrogen deposition is similar for MATCH-BIODIV and MATCH-ECLAIRE, i.e. declining
230 until mid-century. The modelled total deposition in the Scandinavian Mountain area is dominated by oxidized
231 nitrogen, which exhibits a clear decline, while reduced nitrogen deposition levels off at around 2020 and after that
232 even increases slightly for MATCH-BIODIV. These data sets have been evaluated against reanalysis data con-
233 sisting of fused observations and modelled estimates (Andersson et al., Manuscript) for years where all datasets
234 were overlapping (1987-2013) for high-altitude areas of the Scandinavian Mountains. The comparison shows a
235 positive bias in the quantitative modelled total nitrogen deposition by 18% and 23% respectively for the 1987-
236 2013 period, with a stronger positive bias in oxidised nitrogen deposition and a partly balancing negative bias in
237 reduced nitrogen. The trend is similar between the modelled and the reanalysed datasets over the period.

238

239 Historical and RCP8.5 CO_2 concentration data were the same as used by EC-Earth and HCLIM38, reaching at-
240 mospheric concentrations of 540.5 ppm and 935.9 ppm in 2050 and 2100, respectively (IPCC, 2013).

241

242 **2.5 Model output validation and analysis**

243 **2.5.1 Validation**

244 The simulated total leaf-area index (LAI) was compared to the SURFEX LAI product (Masson et al., 2013), taken
245 from ECOCLIMAP2.2 based on MODIS at 1 km resolution in 2000 (Faroux et al., 2013). The modelled LAI for
246 the different PFTs was also converted, to be able to compare, to vegetation classes for two remote-sensing based
247 vegetation products: the land cover of northern Eurasia (GLCE) based on SPOT 4 at 1 km resolution (Bartalev et
248 al., 2003) and the CLC2018 Corine land-cover dataset (Corine) based on Sentinel 2 at 100 m resolution
249 (https://land.copernicus.eu/pan-european/corine-land-cover/clc2018). The conversions (described in detail in S5)
250 were based on Bartalev et al. (2003) and Kosztra et al. (2019) for GLCE and Corine, respectively. The satellite-
251 based products were aggregated to the 3 km AROME gridcells to enable a statistical analysis of the agreement by
252 means of confusion matrixes (e.g. Congalton, 1991), with the satellite products used as ground truth. Three

253 measures of accuracy were calculated. Producer accuracy (PA, probability that a value in a given class was clas-

254 sified correctly, i.e. correctly predicted gridcells of a class / total number of ground truth gridcells in that class),

255 and user accuracy (UA, probability that a value predicted to be in a certain class really is that class, i.e. correctly

256 predicted gridcells of a class / total number of gridcells predicted to be in the class) were calculated for each

257 vegetation class, as well as the overall accuracy (sum of all correctly classified gridcells for all classes / total

258 number of gridcells).

259

260 The model output was also evaluated against ground-based data for biomass (trees and shrubs) and vegetation

261 coverage (field-layer) using data collected in 2011-2012 from four long-term exclosure experiments at Pulsu-

262 vuoma, Ritsem, Långfjället and Fulufjället (for Ritsem only field-layer coverage), all established in 1995 (Figure

263 1a) (Eriksson et al., 2007; Vowles et al., 2017). At each site and vegetation type (birch forest or shrub heath) there

264 were three fenced exclosure plots and three ambient plots of dimension 25 × 25 m. For the gridcells corresponding

265 to these experiments, the model was run both with a) continuous grazing and b) grazing stopped after 1995. To

266 convert model-simulated total biomass C to dry mass, a factor of 2.0 was used (Thomas and Martin, 2012), and

267 to convert modelled total biomass to above ground biomass we assumed a factor of 0.85 based on earlier estimates

268 for Swedish birch forest (between 0.79 and 0.92, Johansson, 2007). The vegetation cover data of the shrub and

269 field layer, visually estimated at species level, were aggregated to the LPJ-GUESS PFTs and compared to simu-

270 lated LAI for 2-3 close gridcells with similar altitude. Though the comparison of fractional plant cover and LAI

271 is not strictly direct, the two measures are closely related (George et al., 2021).

272

273 **2.5.2 Analysis**

274 Due to the more detailed adapted vegetation zones for boreal and Arctic conditions in the GLCE classification,

275 compared to Corine, the future trends presented in the results below focus only on the GLCE data.

276

277 To assess the simulated vegetation diversity, the Shannon (1948) Diversity Index (*D*) was calculated for each of

278 the six "hotspots" (Fig. 1) letting the number of gridcells of different vegetation classes represent diversity:

279 $D = -\sum\left(p_i \times ln(p_i)\right)$           (1)

280 Where *p* is the fraction of the total numbers of classified gridcells in the "hotspot" (excluding prescribed water

281 and wetland cells) belonging to class *i*. Only one vegetation class present would give a *D* of 0 and ten classes with

282 the same *p* would give a value of 2.3.

283

284 The simulated potential reindeer consumption of leaf carbon was aggregated to reindeer herding communities in

285 Sweden for traditional seasonal grazing grounds (Figure 1b), with help of GIS data obtained from the Swedish

286 Sami Parliament (www.sametinget.se).

287

288 **2.6 Biodiversity data**

289 To investigate the sensitivity of the "hotspot" sites to change, species observations of all available species groups

290 together with threatened and red listed species, were extracted for each hotspot area using a GeoJSON file in the

291 "The Analysis portal for biodiversity data" database (downloaded 29th of October 2021. https://www.analysispor-

292 tal.se/). Further, to identify species being classified as alpine, the database "artfakta" (https://artfakta.se/rodlistan)

293 was used with selection criterion "Landscape type" set to "Mountainous".

294

295 **3 Results**

296 **3.1 Validation**

297 **3.1.1 Against satellite-based products**

298 Simulated LAI was lower than in the satellite based SURFEX product but had a reasonable agreement (Figure 2a-

299 b, Simulated_LAI = 0.78 × SURFEX_LAI – 1.99, r^2 = 0.59).

300

301 The simulations capture most of the broad patterns seen in the vegetation distribution from forest to non-vegetated

302 areas when compared to the satellite-based products in 2000 and 2018 (Figure 2c-f). For the detailed classes of

303 the GLCE map the overall accuracy is however only 32% of the gridcells (Table S6a) and for the somewhat wider

304 classes of Corine 37% (Table S6b). Classifying in broader classes, the extent of forest agreed for 84% of gridcells

305 simulated to be forest for both GLCE and Corine (user accuracy, UA) and for 90% and 94% of the satellite-based

306 forest gridcells (producer accuracy, PA) for GLCE and Corine respectively. The most common class of the boreal

307 forest, the needle leaved evergreen forest class, is more mixed with broad-leaved trees in the simulation and the

308 distribution west of the mountains is overestimated compared to the satellite-based products. With the new para-

309 metrization of the IBS PFT (Table S2), the deciduous broad-leaved forest expands too much in the north on the

310 east side of the mountain ranges. Many (30%) of the gridcells that have shrub tundra according to the satellite

311 data were classified as shrub vegetation, resulting in poor UA and PA for those classes in the GLCE comparison.

312 The classes are distinguished based on if the LAI of trees and tall shrubs is more than 20% of the total LAI (Figure

313 S5b). Similarly, for Corine the simulated transitional woodland-shrub class mainly coincides with gridcells clas-

314 sified as broad-leaved forest, moors and heathland, and sparsely vegetated by the satellite product (Figure S5a).

315

316

317

318
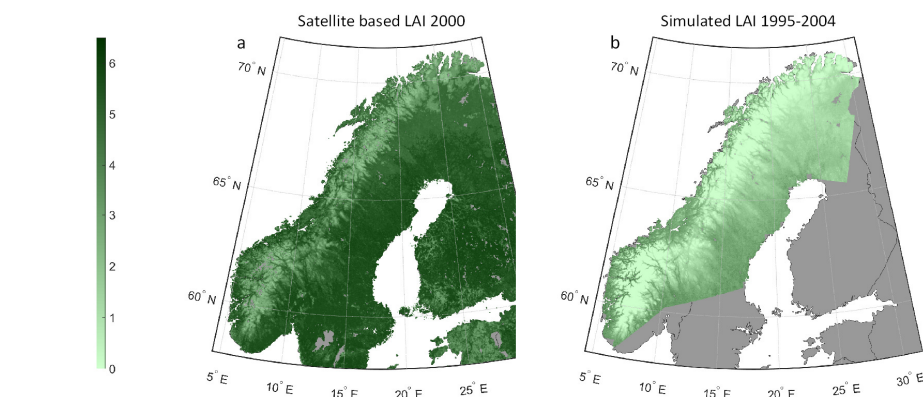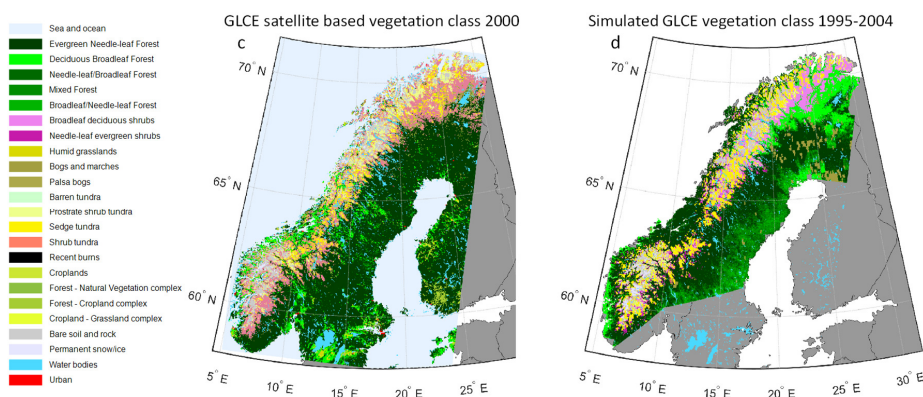
Figure 2. Satellite -based products of LAI (a), GLCE vegetation classes (c), and Corine vegetation classes (e) compared to simulated total LAI (b) and vegetation classes based on LAI for different PFTs according GLC Northern Eurasia (d) and Corine (f) (see Figure S5a-b).

322

Aggregating the tundra classes for GLCE gave a UA of 83% and PA of 36%, where the low PA is the result of many gridcells classified as shrub tundra by the satellite data being simulated to be forest or shrub vegetation. The

"moors and heathland" class is the third largest in the Corine satellite data and was often classified as forest, natural grassland or transitional woodland-shrub by the simulation (UA 18%, PA 4%). The LAI limit for the definition of the bare rock and glacier classes from the simulation were the same for GLCE and Corine classification and both classes were reduced in abundance from 1995-2004 to 2013-2022. The UA and PA for these classes were in the range 11-57%.

3.1.2 Effect of the new reindeer module against vegetation inventories and reindeer exclosures

Comparing model data and the *in-situ* estimated biomass for the northernmost Pulsuvuoma site showed that simulated tree and shrub biomass was underestimated by ca 35% but was within the inventoried uncertainty range of the exclosure site (Figure 3). For the southern sites, biomass was overestimated by ca 50% at Långfjället and by 200% at Fulufjället. A reason for the substantial overestimation for Fulufjället is that it was dominated by needle-leaf trees in the simulation. This was confirmed by test simulations; excluding pine and spruce PFTs (BINE and BNE) reduced biomass with 14%, excluding also the birch PFT (IBS) reduced biomass with 78%.
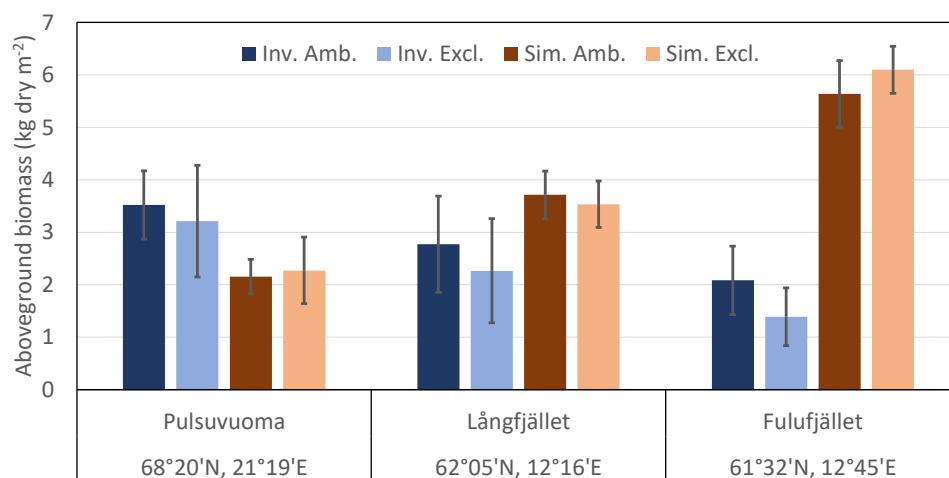
Figure 3. Simulated (Sim., mean over years 2009-2013) aboveground tree and shrub biomass compared to inventoried data (Inv. 2011 or 2012, no biomass data were available for the Ritsem exclosure site) from experiments with ambient plots (Amb.) with reindeer access and plots with exclosure from 1995 (Excl.). Average and standard deviation over 3 inventoried plots or the 2-3 closest simulated gridcells.

The *in-situ* observed coverage of the shrub and field layer from the four exclosure sites was dominated by low evergreen shrubs, mainly *Calluna vulgaris*, *Empetrum nigrum* and *Vaccinium vitis-idaea*, except for the Ritsem shrub heath, which was dominated by graminoids and herbs (Figure S6). The total simulated LAI of the shrub and field layer was low for the two northern sites (0.08 to 0.26 compared to inventoried coverage of 59-75%) and was dominated by graminoids and herbs in the Ritsem shrub heath and high summer-green shrubs below the Pulsuvuoma birch forest. There was a trend that exclosure from reindeer grazing decreased the abundance of graminoids

351   and herbs in both observation and simulations. For the two southern sites, the inventoried coverage and simulated

352   LAI were similar except for Fulufjället, which had a simulated overstory of denser evergreen conifers instead of

353   birch. The trends after exclosure are less clear for the southern sites and the short shrub classes that dominate in

354   the inventories are almost totally absent in the simulations, which are dominated by high shrubs (up to 2m tall),

355   graminoids and herbs. It should be noted that Fulufjället is located outside the area used for reindeer herding,

356   though it is occasionally visited by reindeers from Norway and moose, and the modelling case is hypothetical.

357

3.2 Simulations and analysis of trends in vegetation 2000-2100

3.2.1 Trends over the whole simulated area

360   In the RCP8.5 scenario a dramatic shift in simulated vegetation composition was found, especially after 2050

361   (Figure 4). By 2041-2050 the shrub vegetation classes are already seen to expand to higher elevations in the

362   mountains and the broad-leaved forests in the north start to be mixed with conifers. At the end of the century, the

363   simulated area coverage of open vegetation classes and barren soils were found to be negligible. For instance, the

364   Fennoscandian Low Arctic tundra, which stretches like a wedge from the Kola Peninsula to northernmost Swedish

365   Lapland, in the lee of the mountain chain, would be completely lost by 2100 (Figure 4). Along the southern part

366   of the Norwegian coast and the south-eastern part of the Swedish boreal forest, temperate broadleaf trees (TeBS

367   PFT) start to become dominant in the 2091-2100 period, shown by increasing areas of the deciduous broadleaf

368   class.
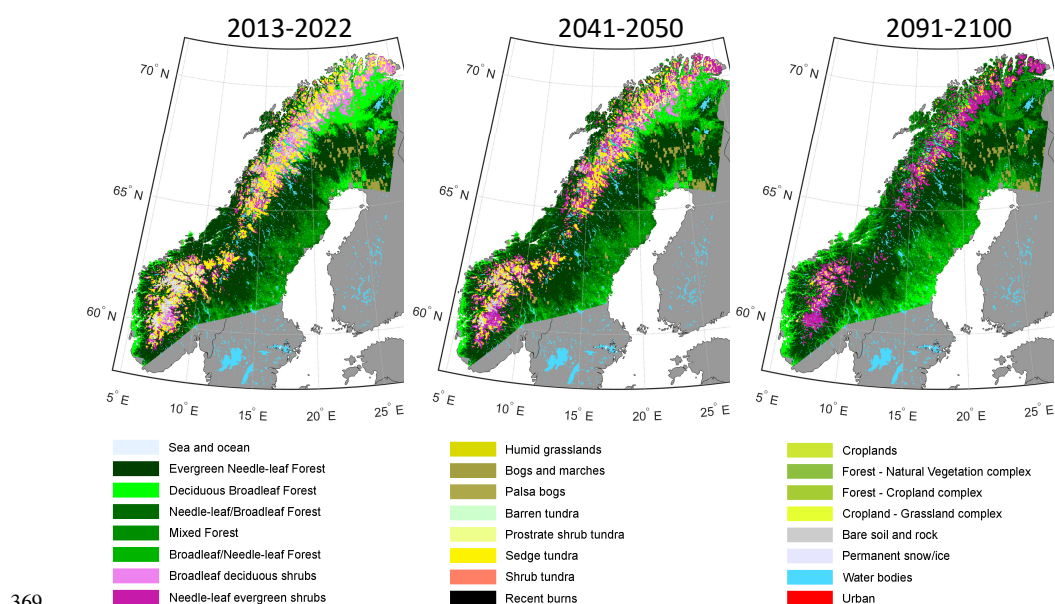
Figure 4. Simulated vegetation classes according to the GLC Northern Eurasia classification based on average LAI for different PFTs over ten years, for three periods in the RCP8.5 scenario.

373 In the western part of the mountains at latitude 68° N, deciduous and mixed forests advance from a simulated
374 current maximum altitude of ca 500 m a.s.l. to more than 1200 m in 2090-2100 (Figure 5). On the east side there
375 is no altitudinal advancement of the forest but a shift from deciduous broad-leaved trees to conifers. Shrub vege-
376 tation classes, especially needle-leaved shrubs, become dominant at mid to high altitudes, for 66° N and 68° N at
377 about 700 to 1200 m and for 61° N less distinctly at 1000 to 1700 m. At latitude 61° N, the lower mountains east
378 of the mountain range become almost completely covered by evergreen needle-leaf forest. The changes seen in
379 the 2041-2050 period are less distinct but the increase in needle-leaved shrubs has started by then, and in the
380 highest elevations a shift in gridcell classification from permanent snow/ice to bare rock can be seen, indicating
381 continued melt of glaciers and snowfields. As the classification is based on LAI, bare rock was set for LAI 0.01-
382 0.001 and permanent snow/ice < 0.001, indicating that plants have the potential to grow there.

383
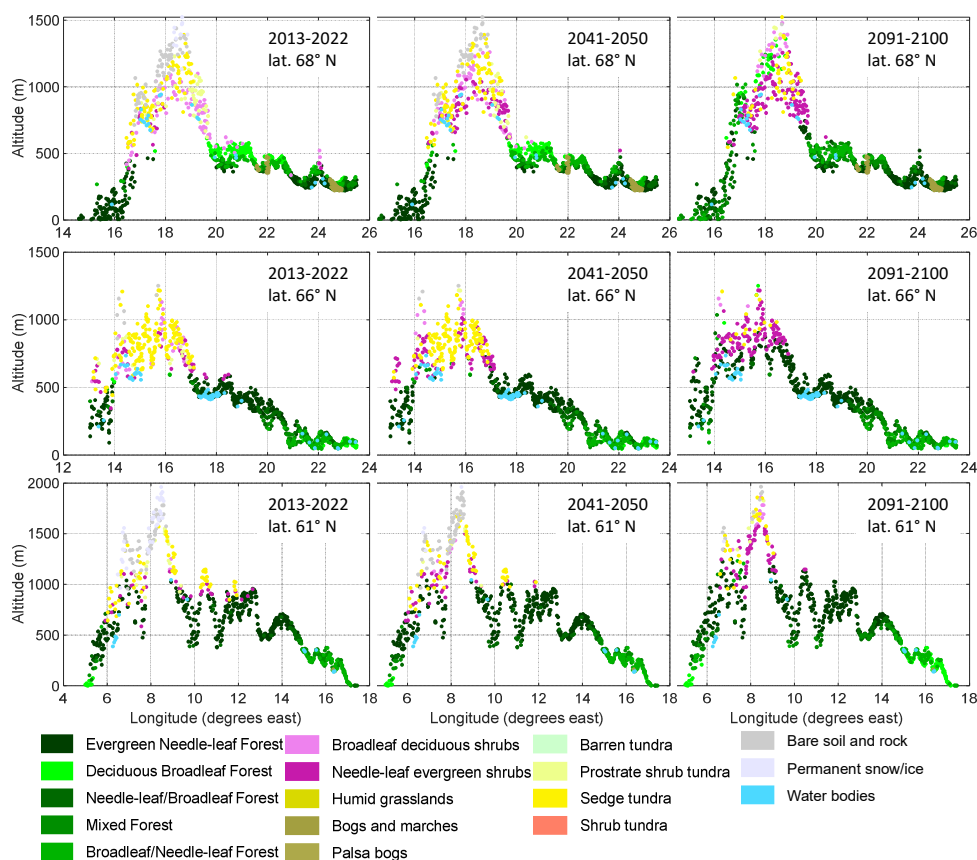
384

385 **Figure 5.** Profiles of simulated vegetation class according to GLCE for the 2013-2022 and RCP8.5 2041-2050 and 2091-2100
386 time periods, shown at the gridcells' longitude and altitude for three latitude bands; 68.0-68.2° N, 66.0-66.15 N° and 61.5-
387 61.6 N°.

388

3.2.2 Detailed analysis with help of empirical data for selected "hotspots"
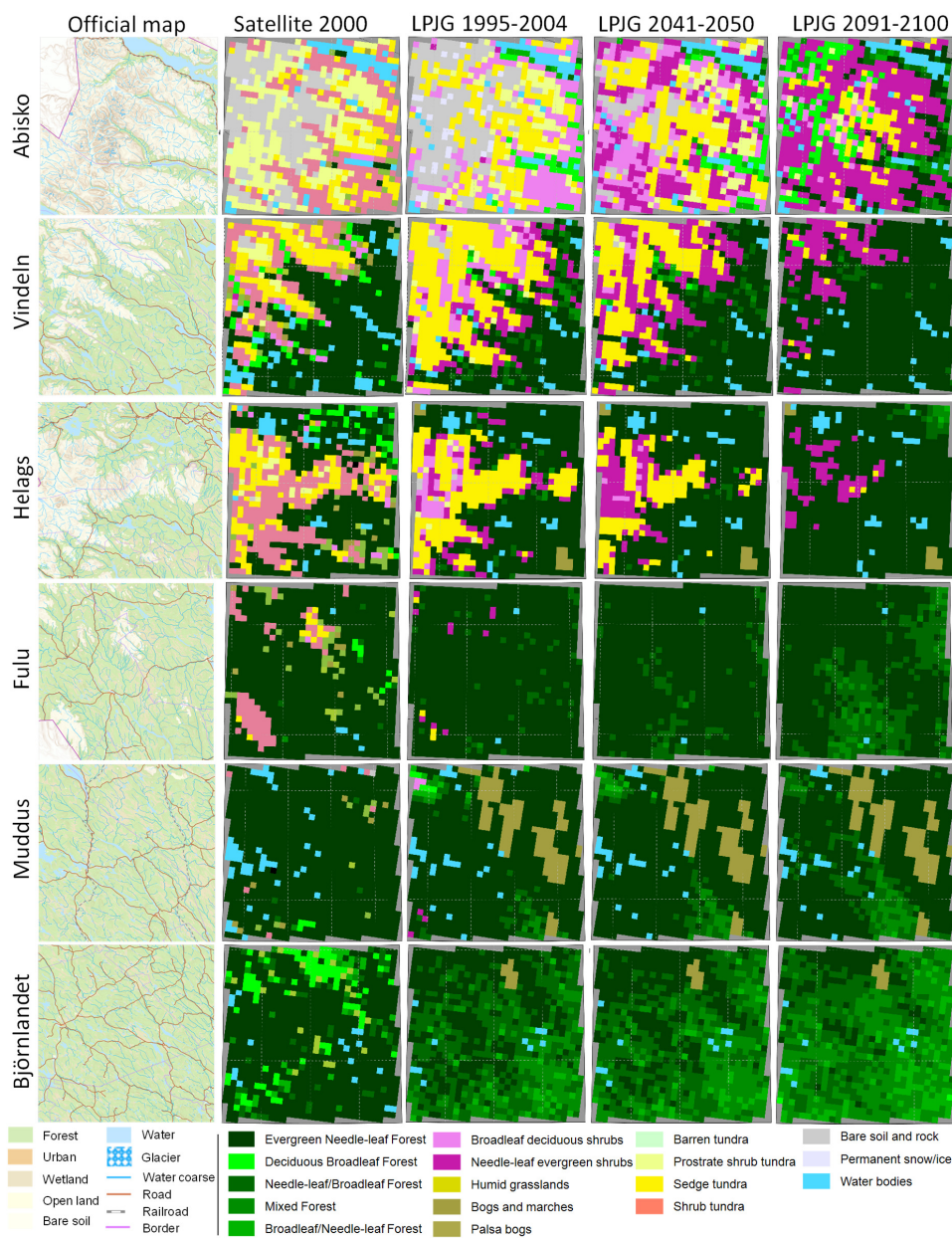
Figure 6. Satellite-based (GLCE, 2nd column) and simulated (column 3-5) vegetation composition in "hotspots" within four mountain areas (row 1-4) and two forest areas (row 5-6) (see Figure 1a for location), for 1995-2004 and for two future periods following RCP8.5. Each area is 90 × 90 km (30 × 30 gridcells). The first column shows the official vector-based map from Lantmäteriet (The overview map, open data license Creative Commons, (CC0), https://www.lantmateriet.se/en/).

395

396 According to the GLCE satellite-based product, the shrub tundra class forms a large fraction of the vegetation
397 next to the boreal needle-leaved forest (Figure 6, Table S7a-d). The official maps from Sweden
398 (https://www.lantmateriet.se/en/maps-and-geographic-information/geodataprodukter/produktlista/oversik-
399 tskartan/) show forest for parts of this area, e.g. in the valleys of the Abisko area.

400

401 For the Vindeln and Helags hotspots, the simulated distribution of forest was close to the satellite-based reference,
402 but for the Fulu hotspot there are just a few gridcells simulated as vegetation other than boreal forest. For
403 Björnlandet the mixture of broad-leaved trees in the forest is of similar magnitude but with a different pattern.
404 The extent of sedge tundra was larger in the simulations than for the GLCE reference for the three northern moun-
405 tain sites.

406

407 By 2041-2050 a significant shrubification occurs in Abisko, Vindeln and Helags (Figure 6), and forests start to
408 establish at the edges of the current shrub and tundra vegetation, an advancement that accelerates until the 2091-
409 2100 period.

410

411 In Abisko the needle-leaf shrub class reached a coverage of approx. 45% of the land area at the end of the century,
412 expanding mainly over former broadleaf shrub, tundra and bare soil classes (Table S7a). In Vindeln and Helags
413 the evergreen needle-leaf forest reaches approx. 80% coverage of the assessed area in 2091-2100 (Table S7b-c).
414 In the boreal forest below the Fulu mountain and in the Muddus and Björnlandet areas, we see that the needle-
415 leaf forest becomes more mixed with broad-leaved trees (Figure 6, Table S7d-f), which is also shown by higher
416 Shannon Diversity Index (D, Table 3). The bog class, which has a large fraction in Muddus, is prescribed from
417 data with 0.125° resolution (see material and methods) and is therefore constant in our simulations.

418

419 For the northernmost hotspot studied, Abisko, the bare soil and rock class will almost disappear in the RCP8.5
420 scenario, but most other classes will remain in similar proportions of the gridcells, though with a shift within the
421 hotspot area (Table S7a). This is reflected in a minor increase in D (Table 3) from 1.69 to 1.75 for this hotspot.
422 Vindeln and Helags will see a clear decrease in diversity as needle leaved forest and shrubs will come to dominate
423 (Table 3). For Fulu and the forests hotspots an increase in diversity is projected as the forests will be more mixed.

424

425 **Table 3.** The Shannon Diversity Index (D) calculated from the fractional cover of GLCE vegetation classes (see S7) of the
426 "hotspots".

	Abisko	Vindeln	Helags	Fulu	Muddus	Björnlandet
Satellite-based class 2000	1.44	1.38	1.42	0.50	0.14	0.80
LPJ-GUESS simulation 1995-2004	1.69	1.72	1.25	0.32	0.50	1.19
LPJ-GUESS simulation 2091-2100	1.75	0.66	0.52	0.83	0.65	1.29

427

428 Vindeln was the area with the lowest number of reported species, whereas Helags was the most diverse area with
429 over 70% more species reported than for Vindeln (Table 4). The four other sites all had fairly equal numbers of

reported species, in the range of 5155-5647 species. However, all hotspots had a similar share of red listed species and threatened species, approximately 8-10% and 3-4%, respectively (Table 4).

Of all threatened species in Sweden (2764 species), only 5.2% (144 species) are classified as alpine and almost 2/3 of these threatened alpine species were found in Abisko, comprising more than half of all the threatened species in Abisko. For Vindeln and Helags, the number of threatened alpine species was just below 20%, whereas the southernmost mountain hotspot Fulu, together with the forest hotspots Muddus and Björnlandet, had less than 10% of their threatened species classified as alpine.

With respect to the species groups to which most of the threatened species belong, it can be noted that mosses contribute the largest number of species in Abisko (Table 4). Except Vindeln, where birds consist of the group with most threatened species, fungi represent the largest number of threatened species for the other four hotspot areas. It should be kept in mind that the data obtained from the Analysis Portal relies on what has been reported by a large community of public and professional naturalists, which means that biases can exist e.g., depending on the specific biological interests of rapporteurs visiting the different areas.

Table 4. Threatened species (VU=vulnerable, EN=endangered, CR=critically endangered) reported across species groups as well as total number of species and red-listed species reported for the six biodiversity hotspot areas.

Species group	Abisko			Vindeln			Helags			Fulu			Muddus			Björnlandet		
	VU	EN	CR	VU	EN	CR	VU	EN	CR	VU	EN	CR	VU	EN	CR	VU	EN	CR
Birds	20	11	3	24	14	3	28	13	3	23	14	3	25	14	4	20	10	2
Fungi	12	2		27	2	1	57	7	1	52	9	4	63	10	2	39	5	
Insects	19	5		22	1		21	6		19	3		37	10		23	11	
Lichens	8	2	1	16	4		29	16	7	24	10	1	14	5		14	4	
Mosses	40	9	1	6	1		33	9		16	6	1	5	3	1	5	2	
Vascular plants	18	7		10	4		17	11	1	26	12	3	8	5		8	1	1
Other groups	1			1	1		2	1		1	1		3	1		2	1	1
Threatened species (% of total)	159	3.1%		137	3.4%		262	3.7%		229	4.4%		210	3.7%		149	2.8%	
of which are alpine species	91	57%		25	18%		51	19%		20	9%		19	9%		9	6%	
Red listed species (% of total)	423	8.2%		369	9.1%		651	9.3%		528	10%		547	9.7%		411	7.8%	
Total reported species	5155			4058			7034			5205			5647			5250		

3.3 Simulations of reindeer presence
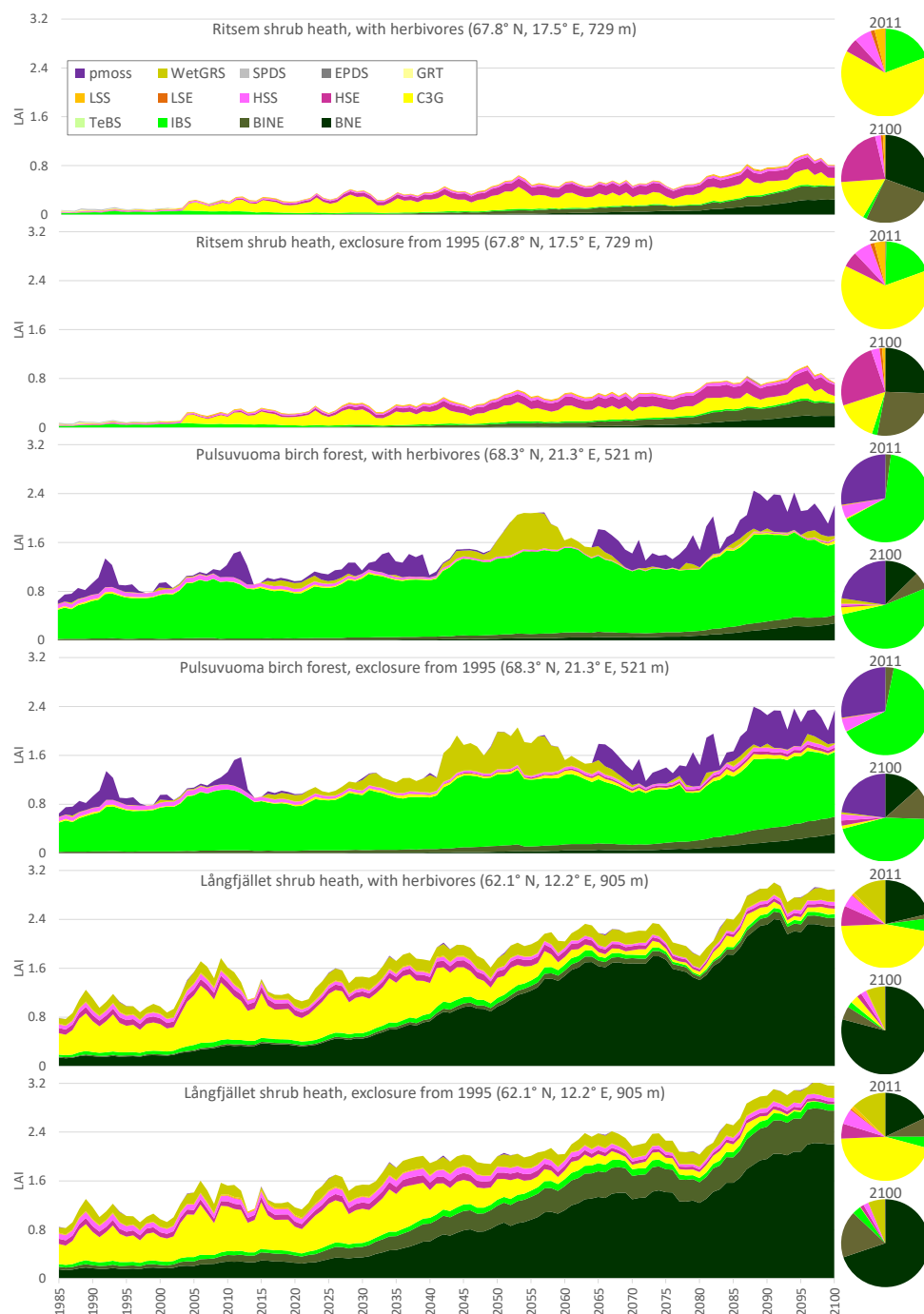
Figure 7. Simulated development of the vegetation composition (based on LAI for different PFTs, see Table 2 for description) at selected gridcells in the exclosure experiments 1985-2100, for RCP8.5.

3.3.1 Effect on vegetation at reindeer exclosure sites

Three gridcells within the exclosure experiments with a wide range of conditions were selected to exemplify the simulated development of the vegetation composition until 2100 (Figure 7). Simulated LAI for the Ritsem shrub heath indicates a steep increase in year 2003, corresponding to an establishment of C3 grass, after which this PFT has a rather constant LAI over the simulation period (Figure 7). Shrub vegetation (PFTs LSS, LSE (both low shrubs), HSS and HSE (tall shrubs)) increases gradually at Ritsem, and, at all sites, shrubs would have a higher fraction without simulated reindeer grazing and trampling.

The mountain birch PFT (IBS) dominates simulations for the Pulsuvuoma birch forest over the simulation period, but for the heath gridcells there is no period with a high fraction of mountain birch forests. Instead PFTs that represent the needle-leaved coniferous forest (BNE and BINE) start to establish at the Ritsem and Pulsuvuoma gridcells around 2035 and these PFTs are already present in the simulations for Långfjället, and at the end of the simulation they are dominant at both shrub heath sites. The summer-green prostrate dwarf shrub PFT (SPDS) has a maximum fraction of ca 50% of LAI at Ritsem, though with a very sparse coverage, before C3 grass takes over, but apart from that, short shrubs (LSS and LSE), prostrate dwarf shrubs (SPDS and EPDS) and the graminoid and forb tundra (GRT) PFTs have only a minor presence in the simulations.

3.3.2 Trends in reindeer grazing 2000-2100

With a constant grazing pressure, simulated reindeer leaf consumption of a PFT depends on available leaf mass, accessibility of the leaves (height less than 2.5 m) and how appetizing it is (preference value – see Table S3). In the current climate the highest consumption was found east of the mountain range with an increasing gradient from north to south (Figure 8).
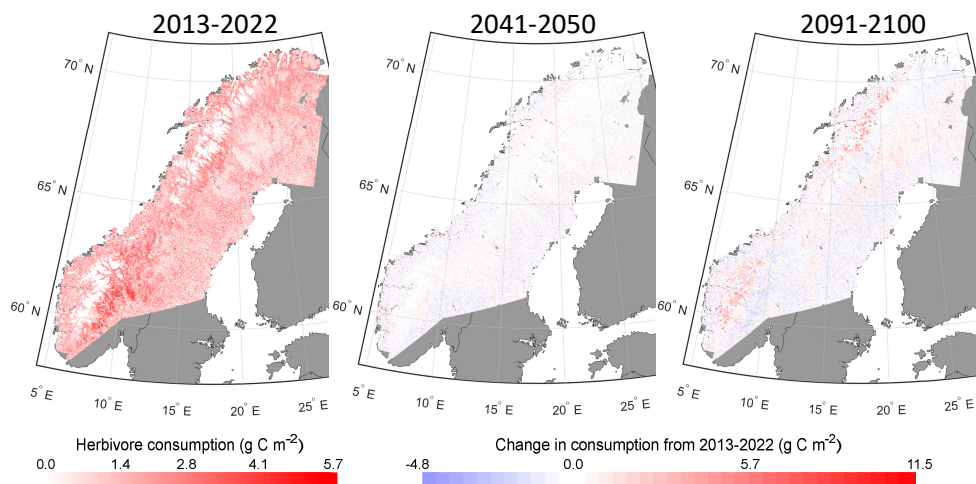
Figure 8. Simulated potential reindeer consumption (g C m^{-2} yr^{-1}) 2013-2022 and the change to 2041-2050 and 2091-2100 in RCP8.5.

480 In the boreal forest zone, the grazing level is quite evenly distributed, though there is a tendency for lower values

481 in areas with a higher fraction of needle-leaf PFTs (Figure 4). The change by the 2041-2050 period is small,

482 though some increased potential in the least vegetated areas can be seen (Figure 8). By the end of the century there

483 is a substantial increase in potential consumption in the higher altitude areas as well as in the inland boreal forest.

484 In the south and towards the east there is a trend towards reduced potential reindeer consumption in the forested

485 cells.

486

487 The traditional spring and autumn grazing grounds of the Swedish reindeer-herding communities overlap to a

488 high degree (Figure 1b) and both have a latitudinal dependency in potential reindeer consumption that is gradually

489 reduced and eventually disappears by the end of the century (Figure 9). For the summer grazing grounds there is

490 a clear latitudinal dependency that is shifted in parallel (i.e. potential consumption increases uniformly) until the

491 2041-2050 period, but by the end of the century the latitudinal trend is gone or becomes negative, with higher

492 potential consumption in the northern part of the study region. For the winter grazing grounds, the latitudinal

493 dependencies are weak and the southern communities have a trend of reduced potential grazing over time. A more

494 detailed compilation of the changes for the individual communities is given in S8.

495
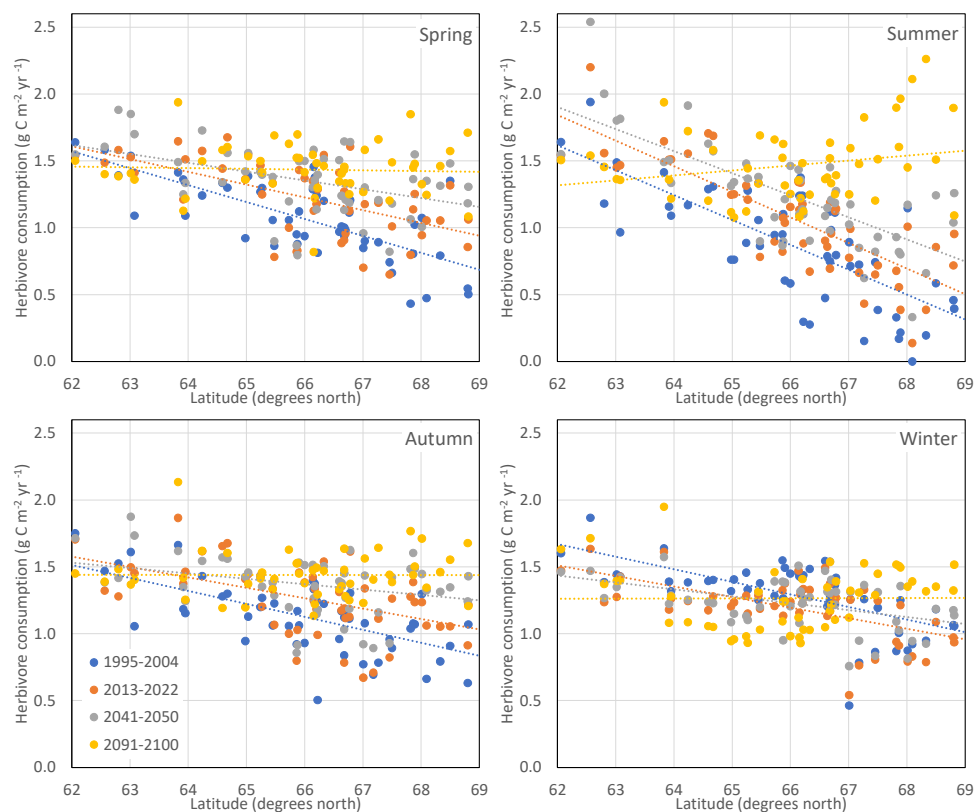
496

497 **Figure 9.** Simulated average potential reindeer consumption of leaf biomass in the 51 reindeer-herding communities in Sweden

498 for the different seasonal grazing grounds (sub picture) and four time periods (colour) in RCP8.5.

499

4 Discussion

501 The simulated changes in vegetation composition at the end of the century are dramatic in our high-emission
502 RCP8.5 scenario. For instance, we see a successive change in forest composition, from a cover of almost purely
503 evergreen trees to a cover containing a larger fraction of broadleaved and mixed forest by the end of the century
504 at the alpine Fulu and low elevation Muddus and Björnlandet hotspots. In Sweden, conifers are highly favoured
505 by forestry for traditional and economic reasons, though pine forest regenerations are already encountering large
506 problems (e.g. from moose grazing and diseases), which can further contribute to an increase of broadleaved
507 forests in the future (Ara et al., 2022). Our results show that a profound vegetation change will occur at the south-
508 ern alpine hotspots Vindeln, Helags, and Fulu, with the most dramatic changes projected for Helags and Vindeln.
509 Here, a rapid tree growth and expansion is observed in this scenario, with only a few tundra-denoted grids remain-
510 ing by 2091-2100. This change is also associated with a strong reduction in landscape diversity, as indicated by a
511 decrease in the vegetation-class based Shannon diversity index. Today, the largest continuous Fennoscandian Low
512 Arctic tundra areas are found between the Swedish high mountains and the border between Finland and Sweden
513 at latitudes around 68.5 °N and in the northern and western parts of the Finnmarksvidda plateau in the north of
514 Norway. In a changed climate, the edges of the tundra area have probably become "Scandinavianized" (Vuorinen
515 et al., 2017), i.e. the coverage of dwarf birches and lichens has decreased, while the *Ericaceae* species have in-
516 creased. The thawing palsas in the area (Luoto and Seppälä, 2003; Olvmo et al., 2020) are also melting faster in
517 area. This is an ecosystem that is extremely vulnerable to the impact of warming, and at high risk of being irre-
518 versibly lost. In the simulations, the tundra remaining in Helags and Vindeln will be dominated by needle-leaf
519 evergreen shrubs with just a few scattered sedge tundra areas (e.g. wet tundra areas). These results are similar to
520 the results from long-term warming experiments and monitoring plots in the northern Scandes, where most com-
521 munities showed a "heathification" with time, both in the experimental warming and under ambient conditions
522 subjected to the ongoing temperature increase (Scharn et al., 2021). At Fulu, the relatively extensive alpine tundra
523 areas are situated just above the tree-line today, and here the tundra will be completely lost following RCP8.5.
524 Thus, with a continued warming of up to 5 K to the end of the century, which is not far from current trend/trajec-
525 tory, the Fennoscandian vegetation will undergo a rapid shift.

526

527 The simulated change in the extent of vegetation zones is driven by establishment of PFTs, but the richness of
528 newly established vegetation depends on the migration of all associated types of organisms. The distance species
529 need to spread to keep up with the shifts in climate is much shorter in mountainous than in flat regions, and since
530 the ability to spread and inhabit new regions varies among species, a loss in species richness only occurs if new
531 immigrants are stronger competitors than the intrinsic species (Pauli and Halloy, 2019). Though total reported
532 species richness is largest in the Helags biodiversity hotspot area and lowest in Vindeln, both have equal fractions
533 of alpine species. As they share the same trajectories, it seems likely that the homogenization of the vegetation
534 composition in the Helags and Vindeln areas will lead to profound shifts in the conditions for many species,
535 especially for the alpine species occurring here. In contrast to the southern alpine hotspots, our modelling results
536 indicate that the northernmost hotspot area Abisko likely will retain large areas of alpine vegetation at higher

537   elevations and its landscape diversity could even slightly increase. A substantial transformation of the vegetation

538   cover is however also expected for Abisko. This includes shrubification, a process that has already been observed

539   in this region (Hedenås et al., 2011; Rundqvist et al., 2011; Scharn et al., 2022; Scharn et al., 2021), and the

540   broadleaved forest moving up well above 1000 m a.s.l. from the current level of about 600-800 m (Callaghan et

541   al., 2013), a treeline advance that also been noted in regional high resolution simulations of Abisko (Gustafson et

542   al., 2021). Abisko is the hotspot with the largest fraction of threatened alpine species in our study, and given the

543   large elevation span in the region there are possibilities that some species may survive in microrefugia (Mee and

544   Moore, 2014). Our results imply that a revision of the red-list and threatened species categories is urgent. This is

545   because many of the alpine species in the hotspots areas that are not listed today will be threatened as warming

546   continues.

547

548   The simulated potential reindeer consumption shows a striking increase in the summer grazing ground north of

549   ca 65.5 °N. Although the simulated potential reindeer consumption is high, it is in the range of what can be

550   estimated from the current reindeer population in Sweden. Today, reindeer husbandry is practiced in about 50%

551   of the Swedish land area (i.e. 225 000 km^2, www.sametinget.se/rennaring_sverige) and the population is 225 000

552   – 280 000 animals in winter (www.sametinget.se/rennaring_sverige). With a consumption of 3-5 kg biomass per

553   reindeer and day (Yu et al., 2017), this equals an average total consumption over the area of about 0.8 g C m^{-2} yr^{-1}

554   ^{1}, a number likely underestimated since as the livestock is larger in summer before autumn slaughter. However,

555   in our simulations of potential reindeer winter consumption, the trends were weak both in latitude and time. Using

556   a constant herbivory intensity in the simulations means that the potential reindeer consumption shown represents

557   a hypothetical case in which we investigate how much would be consumed of the amount that is actually present

558   if the same number of reindeers and the same amount of food of the same quality is present in all gridcells. This

559   means that we have not considered mitigation and adaptation factors that may be of great importance such as

560   climate feedbacks on the population size and changes in what land areas the reindeer feed (Bråthen et al., 2017;

561   Speed et al., 2019). The representation of available reindeer food in the forested winter grazing grounds is chal-

562   lenging. In our simulations, the potential reindeer consumption mainly consists of grasses that occur for a period

563   after the random disturbances (with an average 150-year interval), but grasses are not the preferred reindeer food

564   during winter. Instead, reindeer eat lichens in winter, which naturally can form dense layers under forests in the

565   region. Current forest management, creating a dense and uniform tree cover, disturbs the growth of lichens

566   (Kumpula et al., 2014). Furthermore, our weak trends during winter also depend on a delicate balance between a

567   general increased productivity and higher density of the tree canopies. This balance is also important for the im-

568   plementation of ground lichen PFTs, since there is a negative relationship between forest density and lichen abun-

569   dance (Sandström et al., 2016). Thus, future improvements to simulations considering reindeer grazing would

570   need: a better representation of winter forage by developing a new lichen PFT (e.g. Porada et al., 2016); an im-

571   proved light-interception scheme; forest management functionality and scenarios (e.g. Lindeskog et al., 2021);

572   and a representation of restricted access to the field and bottom layer vegetation during periods of difficult snow

573   conditions. Though the simulated potential reindeer consumption does not show dramatic shifts over the simulated

574   period, reindeer herding will nevertheless experience climate and weather related challenges in the future with

575   e.g. concerns for hot and dry summers, more frequent freeze-thaw cycles and rain-on snow events during winters,

576   as well as expanding and denser forests (Käyhkö and Horstkotte, 2017; Rosqvist et al., 2021). Thus, to be able to

577 tackle and understand future challenges for reindeer herding this not only suggests a need to include trophic in-
578 teractions in models, but it also suggests that it is crucial to evaluate the impact of extreme events on other im-
579 portant aspects of the environment for reindeer herding than vegetation state alone.

581 We show the benefit of using high-resolution climate data to drive our DVM, enabling the simulation of a diverse
582 landscape, exemplified by our hotspot analysis (which would have less than 4 gridcells at a typical RCM resolution
583 of 50×50 km). Climate representation has also improved. In particular, the simulated precipitation patterns in
584 coastal and mountain areas as well as the ratio between snow and rainfall at high altitude show significantly better
585 agreement with observations at higher resolutions (Lind et al., 2020). Thus, highly resolved climate data in com-
586 bination with a state-of-the-art dynamical vegetation model clearly contributes to a better understanding of cli-
587 mate-vegetation interactions in mountainous regions. There is, however, uncertainty at many levels in this type of
588 study: What emission scenario will the future follow and is it adequately interpreted by the global and regional
589 climate models? Is the vegetation's direct response to climate, CO_2 concentration, and nitrogen deposition ade-
590 quately described in the DVM? How will secondary effects of climate change alter disturbance patterns and land
591 use? Due to computational limitations in this high-resolution application, it has not been possible to quantify these
592 uncertainties (e.g. we only have one climate scenario), but it is clear from earlier studies and our results that all
593 these aspects are important. The direction in which the results point is, however, clear in most aspects.

595 Using the detailed classification from GLCE, the accuracy scores for the simulated vegetation classes compared
596 to the satellite product are low. For such a large area and high resolution as in the present study, an evaluation
597 against satellite products is the only alternative with a complete coverage, but the satellite classes cannot be con-
598 sidered a real "ground truth". An example of possible misclassification of the GLCE data is clear from the fact
599 that the mountain-birch forest in some of the valleys is classified as shrub vegetation, most clearly seen for Abisko
600 and Vindeln when compared to the official vector-based maps. The shrub and tundra ecosystems have many
601 subclasses and the model has some difficulty in reproducing the satellite-based pattern for these. Furthermore, the
602 parameterization of the PFTs representing these systems is based on global or regional implementations driven
603 by monthly climate data at coarse spatial scale (Wolf et al., 2008; Zhang et al., 2013), and it is not surprising that
604 the results call for some model adjustment. A further limitation of the vegetation simulations is that a soil layer
605 always is present. The strong expansion of shrubs on former "bare soil & rock" and "permanent snow/ice" classes,
606 e.g. as predicted for the Abisko area, is, therefore, probably overestimated, and instead parts of this area would
607 become some type of tundra associated with shallow soils. Dispersal capacity and fire disturbance are also factors
608 that may restrict vegetation expansion, as integration of those processes in an extrapolation of current trends in
609 Alaska and western Canada reduced the predicted shrub expansion on non-shrub tundra from 39 to 25% by 2100
610 (Liu et al., 2022). There is also a positive bias in the nitrogen deposition scenario (Andersson et al., 2023, manu-
611 script) that could have further enhanced the simulated rate at which higher vegetation types expand (Gustafson et
612 al., 2021). In the boreal forest region, the simulations have a higher fraction of broadleaf trees than the reference.
613 A reason for this is that more than 90% of these forests are managed and needle-leaved trees are favoured in
614 planting and thinning (Hannerz and Ekström, 2021) whereas the simulations represent natural, unmanaged vege-
615 tation where broadleaf trees are common during the regeneration phase after disturbances in boreal forest
616 (Angelstam and Kuuluvainen, 2004). However, notwithstanding these limitations, our simulations clearly show

617 that for Fennoscandia, the RCP8.5 pathway results in more prominent temperate features in the boreal forest, and

618 that these will expand northwards and to higher altitude resulting in a significant loss in tundra.

619

5 Conclusion

621 Our application of highly resolved climate data greatly improved both the representation of climate conditions

622 and the variation in simulated vegetation in mountainous landscapes. Climate and environmental change con-

623 sistent with the high-emission RCP8.5 scenario could cause dramatic shifts in the vegetation composition of the

624 Fennoscandian boreal and mountain regions, with consequences for our society, and implications for recreation,

625 how we should practise conservation, and how we should manage our northern ecosystems. Indeed, these changes

626 have already started and been observed, but they will accelerate during the 21st century. Following a climate

627 trajectory in line with RCP8.5, the southern and lower elevation parts of the Fennoscandian mountain range that

628 today have tundra vegetation will be covered by forests in the coming century, while high-elevation regions will

629 undergo intense shrubification. In the northern tundra regions, most vegetation types will still be present at the

630 end of the century but shift in altitude and be compressed to smaller regions. This will threaten already vulnerable

631 species, especially those with slow dispersal rates and low competitive ability. In the southern part of the study

632 area a massive loss of alpine habitats and species is expected. The question is rather what new vegetation types

633 and species could occupy this area under continued climate change. The rate of actual vegetation changes will

634 also depend on factors such as forest management, reindeer husbandry, other disturbances (such as fire) and the

635 dispersal rate of different species. Our results indicate trends towards increasing amounts of suitable reindeer

636 forage, at least in northern Sweden, but other changes resulting from climate change, such as the extent of open

637 landscapes, heat stress and altered snow conditions are likely to impact reindeer herding practises more than forage

638 availability. The expected and potentially additive pressures of environmental changes call for scenario-based

639 research where the main drivers of the development, including climate change, air pollution, land use and ecolog-

640 ical processes, are considered in a consistent framework.

641

Code availability

643 The LPJ-GUESS code used and developed in this study is archived in the LPJ-GUESS Community Repository

644 on Zenodo: https://zenodo.org/record/8262590 (Lagergren et al., 2023). More information about the model can

645 be found at https://web.nateko.lu.se/lpj-guess (LPJ-GUESS developers, 2021).

646

Data availability

648 A selection of the MATCH-BIODIV dataset and the MATCH-ECLAIRE (Engardt et al., 2017) datasets are ar-

649 chived in Zenodo (MATCH-BIODIV: https://zenodo.org/record/7573171 and MATCH-ECLAIRE: https://ze-

650 nodo.org/record/4501636#.ZBqvOXbMJaQ). The ALADIN and AROME H-CLIM climate datasets (Lind et al.,

651 2022), and the complete MATCH-BIODIV nitrogen deposition dataset (Andersson et al., 2023, manuscript) were

generously shared with the authors but are not publicly accessible; the data can be accessed upon inquiry to the authors. The ECLIPSE V6b nitrogen deposition data are available from IIASA (https://previ-ous.iiasa.ac.at/web/home/research/researchPrograms/air/ECLIPSEv6b.html) and the NGCD data used for bias correction of temperature can be accessed at the MET Norway Thredds Service (https://thredds.met.no/thredds/catalog/ngcd/catalog.html). The FAO soil texture data are available at the SURFEX site (https://www.umr-cnrm.fr/surfex/spip.php?article135). The Corine land-cover data (https://land.co-pernicus.eu/pan-european/corine-land-cover/clc2018) and the GLCE product for northern Eurasia (https://forobs.jrc.ec.europa.eu/products/glc2000/products.php) are freely available. The GIS data of reindeer herding communities were obtained after personal contact with Peter Benson from the Swedish Sami Parliament (www.sametinget.se) but are not freely available. Vegetation cover data (Vowles et al., 2017) can be accessed through Environment Climate Data Sweden (https://doi.org/10.5879/ECDS/2017-01-29.1/0). The biomass data from the exclosure sites are not available to the public but can be accessed by personal contact with the authors (R. Björk). Species observations for the hotspots are available at "The Analysis portal for biodiversity data" da-tabase (https://www.analysisportal.se/). Model simulation results with LPJ-GUESS for this manuscript are stored on DataGURU: https://dataguru.lu.se/app#BioDiv-S (Lagergren and Miller, 2023).

Author contribution

FL and PAM designed the study with contribution from RGB, CA, MPB, EK, HP and GR. FL carried out the vegetation model development, setup, runs and data analysis with support from PAM. RGB extracted and analysed the biodiversity data with help from MPB and HP. DB, PL and DL provided the climate scenario and associated soil and vegetation attributes. CA and TO provided high-resolution nitrogen deposition data. FL carried out bias correction and filling of continuous climate and nitrogen deposition data with advice from DB, EK and CA. RGB, MPB and GR contributed with expertise in reindeer husbandry and its interaction with the vegetation. FL prepared the manuscript with input from all co-authors.

Short summary

The Fennoscandian boreal and mountain regions harbour a wide range of ecosystems sensitive to climate change. A new, highly resolved high-emission climate scenario enabled modelling of the vegetation development in this region at high resolution for the 21st century. The results show dramatic south to north and low to high altitude shifts of vegetation zones, especially for the open tundra environments, that will have large implications for nature conservation, reindeer husbandry and forestry.

Acknowledgement

This work was supported by the BioDiv-Support project funded through the 2017-2018 Belmont Forum and Bi-odivERsA joint call for research proposals, under the BiodivScen ERA-Net COFUND programme, and with the

687   funding organisations AKA (contract no 326328), ANR (ANR-18-EBI4-0007), BMBF (KFZ: 01LC1810A),

688   FORMAS (contract no:s 2018-02434, 2018-02436, 2018-02437, 2018-02438) and MICINN (through APCIN:

689   PCI2018-093149). The work is a contribution to the strategic research areas MERGE and BECC, and the profile

690   area Nature-based Future Solutions hosted by Lund University. We thank Peter Benson at Sametinget for provid-

691   ing data of the reindeer husbandry districts in Sweden and Mora Aronsson, Debora Arlt, and Johan Nilsson for

692   advice regarding the extraction of data from the "The Analysis portal for biodiversity data".

693

694   **References**

695   Andersson, C., Langner, J., and Bergström, R.: Interannual variation and trends in air pollution over Europe due

696   to climate variability during 1958-2001 simulated with a regional CTM coupled to the ERA40 reanalysis, Tellus

697   Series B-Chemical and Physical Meteorology, 59, 77-98, https://doi.org/10.1111/j.1600-0889.2006.00231.x,

698   2007.

699   Andersson, C., Bergström, R., Bennet, C., Robertson, L., Thomas, M., Korhonen, H., Lehtinen, K. E. J., and

700   Kokkola, H.: MATCH-SALSA - Multi-scale Atmospheric Transport and CHemistry model coupled to the SALSA

701   aerosol microphysics model - Part 1: Model description and evaluation, Geoscientific Model Development, 8,

702   171-189, https://doi.org/10.5194/gmd-8-171-2015, 2015.

703   Andersson, C., Olenius, T., Alpfjord Wylde, H., Almroth Rosell, E., Björk, R. G., Björkman, M. P., Moldan, F.,

704   and Engardt, M.: Long-term nitrogen deposition to northern Europe with focus on the Baltic Sea and the

705   Scandinavian Mountains: reanalysis for the years 1983-2013 and comparison to multi-century (1900-2051) model

706   simulations, Manuscript.

707   Angelstam, P. and Kuuluvainen, T.: Boreal forest disturbance regimes, successional dynamics and landscape

708   structures - a European perspective, Ecological Bulletins, 51, 117-136, https://doi.org/10.2307/20113303, 2004.

709   Ara, M., Barbeito, I., Kalén, C., and Nilsson, U.: Regeneration failure of Scots pine changes the species

710   composition of young forests, Scandinavian Journal of Forest Research, 37, 14-22,

711   https://doi.org/10.1080/02827581.2021.2005133, 2022.

712   Bartalev, S. A., Belward, A. S., Erchov, D. V., and Isaev, A. S.: A new SPOT4-VEGETATION derived land

713   cover map of Northern Eurasia, International Journal of Remote Sensing, 24, 1977-1982,

714   https://doi.org/10.1080/0143116031000066297, 2003.

715   Barthelemy, H., Stark, S., Michelsen, A., and Olofsson, J.: Urine is an important nitrogen source for plants

716   irrespective of vegetation composition in an Arctic tundra: Insights from a N-15-enriched urea tracer experiment,

717   Journal of Ecology, 106, 367-378, https://doi.org/10.1111/1365-2745.12820, 2018.

718   Belušić, D., de Vries, H., Dobler, A., Landgren, O., Lind, P., Lindstedt, D., Pedersen, R. A., Sánchez-Perrino, J.

719   C., Toivonen, E., van Ulft, B., Wang, F. X., Andrae, U., Batrak, Y., Kjellström, E., Lenderink, G., Nikulin, G.,

720 Pietikäinen, J. P., Rodríguez-Camino, E., Samuelsson, P., van Meijgaard, E., and Wu, M. C.: HCLIM38: a flexible
721 regional climate model applicable for different climate zones from coarse to convection-permitting scales,
722 Geoscientific Model Development, 13, 1311-1333, https://doi.org/10.5194/gmd-13-1311-2020, 2020.

723 Bjorkman, A. D., García, C. M., Myers-Smith, I. H., Ravolainen, V., Svala Jónsdóttir, I., Westergaard, K. B.,
724 Lawler, J. P., Aronsson, M., Bennett, B., Gardfjell, H., Heiðmarsson, S., Stewart, L., and Normand, S.: Status and
725 trends in Arctic vegetation: Evidence from experimental warming and long-term monitoring, Ambio, 49, 678-
726 692, https://doi.org/10.1007/s13280-019-01161-6, 2020.

727 Bjorkman, A. D., Myers-Smith, I. H., Elmendorf, S. C., Normand, S., Rueger, N., Beck, P. S. A., Blach-
728 Overgaard, A., Blok, D., Cornelissen, J. H. C., Forbes, B. C., Georges, D., Goetz, S. J., Guay, K. C., Henry, G. H.
729 R., HilleRisLambers, J., Hollister, R. D., Karger, D. N., Kattge, J., Manning, P., Prevey, J. S., Rixen, C.,
730 Schaepman-Strub, G., Thomas, H. J. D., Vellend, M., Wilmking, M., Wipf, S., Carbognani, M., Hermanutz, L.,
731 Levesque, E., Molau, U., Petraglia, A., Soudzilovskaia, N. A., Spasojevic, M. J., Tomaselli, M., Vowles, T.,
732 Alatalo, J. M., Alexander, H. D., Anadon-Rosell, A., Angers-Blondin, S., te Beest, M., Berner, L., Bjork, R. G.,
733 Buchwal, A., Buras, A., Christie, K., Cooper, E. J., Dullinger, S., Elberling, B., Eskelinen, A., Frei, E. R., Grau,
734 O., Grogan, P., Hallinger, M., Harper, K. A., Heijmans, M. M. P. D., Hudson, J., Huelber, K., Iturrate-Garcia, M.,
735 Iversen, C. M., Jaroszynska, F., Johnstone, J. F., Jorgensen, R. H., Kaarlejarvi, E., Klady, R., Kuleza, S., Kulonen,
736 A., Lamarque, L. J., Lantz, T., Little, C. J., Speed, J. D. M., Michelsen, A., Milbau, A., Nabe-Nielsen, J., Nielsen,
737 S. S., Ninot, J. M., Oberbauer, S. F., Olofsson, J., Onipchenko, V. G., Rumpf, S. B., Semenchuk, P., Shetti, R.,
738 Collier, L. S., Street, L. E., Suding, K. N., Tape, K. D., Trant, A., Treier, U. A., Tremblay, J.-P., Tremblay, M.,
739 Venn, S., Weijers, S., Zamin, T., Boulanger-Lapointe, N., Gould, W. A., Hik, D. S., Hofgaard, A., Jonsdottir, I.
740 S., Jorgenson, J., Klein, J., Magnusson, B., Tweedie, C., Wookey, P. A., Bahn, M., Blonder, B., van Bodegom, P.
741 M., Bond-Lamberty, B., Campetella, G., Cerabolini, B. E. L., Chapin, F. S., III, Cornwell, W. K., Craine, J.,
742 Dainese, M., de Vries, F. T., Diaz, S., Enquist, B. J., Green, W., Milla, R., Niinemets, U., Onoda, Y., Ordonez, J.
743 C., Ozinga, W. A., Penuelas, J., Poorter, H., Poschlod, P., Reich, P. B., Sande, B., Schamp, B., Sheremetev, S.,
744 and Weiher, E.: Plant functional trait change across a warming tundra biome, Nature, 562, 57-62,
745 https://doi.org/10.1038/s41586-018-0563-7, 2018.

746 Bråthen, K. A., Ravolainen, V. T., Stien, A., Tveraa, T., and Ims, R. A.: Rangifer management controls a climate-
747 sensitive tundra state transition, Ecological Applications, 27, 2416-2427, https://doi.org/10.1002/eap.1618, 2017.

748 Callaghan, T. V., Gatti, R. C., and Phoenix, G.: The need to understand the stability of arctic vegetation during
749 rapid climate change: An assessment of imbalance in the literature, Ambio, 51, 1034-1044,
750 https://doi.org/10.1007/s13280-021-01607-w, 2022.

751 Callaghan, T. V., Jonasson, C., Thierfelder, T., Yang, Z., Hedenås, H., Johansson, M., Molau, U., Van Bogaert,
752 R., Michelsen, A., Olofsson, J., Gwynn-Jones, D., Bokhorst, S., Phoenix, G., Bjerke, J. W., Tømmervik, H.,
753 Christensen, T. R., Hanna, E., Koller, E. K., and Sloan, V. L.: Ecosystem change and stability over multiple
754 decades in the Swedish subarctic: complex processes and multiple drivers, Philosophical Transactions of the
755 Royal Society B-Biological Sciences, 368, 20120488, https://doi.org/10.1098/rstb.2012.0488, 2013.

756   Congalton, R. G.: A review of assessing the accuracy of classifications of remotely sensed data, Remote Sensing
757   of Environment, 37, 35-46, https://doi.org/10.1016/0034-4257(91)90048-b, 1991.

758   Constable, A. J., Harper, S., Dawson, J., Holsman, K., Mustonen, T., Piepenburg, D., and Rost, B.: Cross-Chapter
759   Paper 6: Polar Regions, in: Climate Change 2022: Impacts, Adaptation and Vulnerability. Contribution of
760   Working Group II to the Sixth Assessment Report of the Intergovernmental Panel on Climate Change, edited by:
761   Pörtner, H.-O., Roberts, D. C., Tignor, M., Poloczanska, E. S., Mintenbeck, K., Alegría, A., Craig, M., Langsdorf,
762   S., Löschke, S., Möller, V., Okem, A., and Rama, B., Cambridge University Press,, Cambridge, UK and New
763   York, NY, USA,, 2319-2368, https://doi.org/10.1017/9781009325844.023, 2022.

764   Denryter, K. A., Cook, R. C., Cook, J. G., and Parker, K. L.: Straight from the caribou's (Rangifer tarandus)
765   mouth: detailed observations of tame caribou reveal new insights into summer-autumn diets, Canadian Journal of
766   Zoology, 95, 81-94, https://doi.org/10.1139/cjz-2016-0114, 2017.

767   Egelkraut, D., Barthelemy, H., and Olofsson, J.: Reindeer trampling promotes vegetation changes in tundra
768   heathlands: Results from a simulation experiment, Journal of Vegetation Science, 31, 476-486,
769   https://doi.org/10.1111/jvs.12871, 2020.

770   Eichler, A., Legrand, M., Jenk, T. M., Preunkert, S., Andersson, C., Eckhardt, S., Engardt, M., Plach, A., and
771   Schwikowski, M.: Consistent histories of anthropogenic western European air pollution preserved in different
772   Alpine ice cores, The Cryosphere, 17, 2119-2137, https://doi.org/10.5194/tc-17-2119-2023, 2023.

773   Elmendorf, S. C., Henry, G. H. R., Hollister, R. D., Björk, R. G., Boulanger-Lapointe, N., Cooper, E. J.,
774   Cornelissen, J. H. C., Day, T. A., Dorrepaal, E., Elumeeva, T. G., Gill, M., Gould, W. A., Harte, J., Hik, D. S.,
775   Hofgaard, A., Johnson, D. R., Johnstone, J. F., Jonsdottir, I. S., Jorgenson, J. C., Klanderud, K., Klein, J. A., Koh,
776   S., Kudo, G., Lara, M., Levesque, E., Magnusson, B., May, J. L., Mercado-Diaz, J. A., Michelsen, A., Molau, U.,
777   Myers-Smith, I. H., Oberbauer, S. F., Onipchenko, V. G., Rixen, C., Schmidt, N. M., Shaver, G. R., Spasojevic,
778   M. J., Porhallsdottir, P. E., Tolvanen, A., Troxler, T., Tweedie, C. E., Villareal, S., Wahren, C.-H., Walker, X.,
779   Webber, P. J., Welker, J. M., and Wipf, S.: Plot-scale evidence of tundra vegetation change and links to recent
780   summer warming, Nature Climate Change, 2, 453-457, https://doi.org/10.1038/nclimate1465, 2012.

781   Engardt, M., Simpson, D., Schwikowski, M., and Granat, L.: Deposition of sulphur and nitrogen in Europe 1900-
782   2050. Model calculations and comparison to historical observations, Tellus Series B-Chemical and Physical
783   Meteorology, 69, 1328945, https://doi.org/10.1080/16000889.2017.1328945, 2017.

784   Eriksson, O., Niva, M., and Caruso, A.: Use and abuse of reindeer range, Acta Phytogeographica Suecica, 87, 1-
785   110, 2007.

786   Faroux, S., Kaptué Tchuenté, A. T., Roujean, J.-L., Masson, V., Martin, E., and Le Moigne, P.: ECOCLIMAP-
787   II/Europe: a twofold database of ecosystems and surface parameters at 1 km resolution based on satellite
788   information for use in land surface, meteorological and climate models, Geoscientific Model Development, 6,
789   563-582, https://doi.org/10.5194/gmd-6-563-2013, 2013.

790   Feeley, K. J., Silman, M. R., Bush, M. B., Farfan, W., Cabrera, K. G., Malhi, Y., Meir, P., Revilla, N. S.,
791   Quisiyupanqui, M. N. R., and Saatchi, S.: Upslope migration of Andean trees, Journal of Biogeography, 38, 783-
792   791, https://doi.org/10.1111/j.1365-2699.2010.02444.x, 2011.

793   Ferraro, K. M., Schmitz, O. J., and McCary, M. A.: Effects of ungulate density and sociality on landscape
794   heterogeneity: a mechanistic modeling approach, Ecography, 2022, e06039, https://doi.org/10.1111/ecog.06039,
795   2022.

796   Fohringer, C., Rosqvist, G., Inga, N., and Singh, N. J.: Reindeer husbandry in peril?-How extractive industries
797   exert   multiple   pressures   on   an   Arctic   pastoral   ecosystem,   People   and   Nature,   3,   872-886,
798   https://doi.org/10.1002/pan3.10234, 2021.

799   George, J.-P., Yang, W., Kobayashi, H., Biermann, T., Carrara, A., Cremonese, E., Cuntz, M., Fares, S., Gerosa,
800   G., Grünwald, T., Hase, N., Heliasz, M., Ibrom, A., Knohl, A., Kruijt, B., Lange, H., Limousin, J.-M., Loustau,
801   D., Lukeš, P., Marzuoli, R., Mölder, M., Montagnani, L., Neirynck, J., Peichl, M., Rebmann, C., Schmidt, M.,
802   Serrano, F. R. L., Soudani, K., Vincke, C., and Pisek, J.: Method comparison of indirect assessments of understory
803   leaf area index (LAI(u)): A case study across the extended network of ICOS forest ecosystem sites in Europe,
804   Ecological Indicators, 128, https://doi.org/10.1016/j.ecolind.2021.107841, 2021.

805   Gustafson, A., Miller, P. A., Björk, R., Olin, S., and Smith, B.: Nitrogen restricts future treeline advance in the
806   sub-arctic, Biogeosciences, 18, 6329–6347, https://doi.org/10.5194/bg-2021-169, 2021.

807   Hannerz, M. and Ekström, H.: Nordic Forest Statistics 2020 – Resources, Industry, Trade, Conservation, and
808   Climate, Nordic Forest Research, 32, 2021.

809   Hazeleger, W., Wang, X., Severijns, C., Ştefănescu, S., Bintanja, R., Sterl, A., Wyser, K., Semmler, T., Yang, S.,
810   van den Hurk, B., van Noije, T., van der Linden, E., and van der Wiel, K.: EC-Earth V2.2: description and
811   validation   of   a   new   seamless   earth   system   prediction   model,   Climate   Dynamics,   39,   2611-2629,
812   https://doi.org/10.1007/s00382-011-1228-5, 2012.

813   Hazeleger, W., Severijns, C., Semmler, T., Ştefănescu, S., Yang, S., Wang, X., Wyser, K., Dutra, E., Baldasano,
814   J. M., Bintanja, R., Bougeault, P., Caballero, R., Ekman, A. M. L., Christensen, J. H., van den Hurk, B., Jimenez,
815   P., Jones, C., Kållberg, P., Koenigk, T., McGrath, R., Miranda, P., Van Noije, T., Palmer, T., Parodi, J. A.,
816   Schmith, T., Selten, F., Storelvmo, T., Sterl, A., Tapamo, H., Vancoppenolle, M., Viterbo, P., and Willén, U.: EC-
817   Earth A Seamless Earth-System Prediction Approach in Action, Bulletin of the American Meteorological Society,
818   91, 1357-1363, https://doi.org/10.1175/2010bams2877.1, 2010.

819   Hedenås, H., Olsson, H., Jonasson, C., Bergstedt, J., Dahlberg, U., and Callaghan, T. V.: Changes in Tree Growth,
820   Biomass   and   Vegetation   Over   a   13-Year   Period   in   the   Swedish   Sub-Arctic,   Ambio,   40,   672-682,
821   https://doi.org/10.1007/s13280-011-0173-1, 2011.

822   Hickler, T., Vohland, K., Feehan, J., Miller, P. A., Smith, B., Costa, L., Giesecke, T., Fronzek, S., Carter, T. R.,
823   Cramer, W., Kühn, I., and Sykes, M. T.: Projecting the future distribution of European potential natural vegetation

zones with a generalized, tree species-based dynamic vegetation model, Global Ecology and Biogeography, 21, 50-63, https://doi.org/10.1111/j.1466-8238.2010.00613.x, 2012.

Höglund-Isaksson, L., Gómez-Sanabria, A., Klimont, Z., Rafaj, P., and Schöpp, W.: Technical potentials and costs for reducing global anthropogenic methane emissions in the 2050 timeframe -results from the GAINS model, Environmental Research Communications, 2, 025004, https://doi.org/10.1088/2515-7620/ab7457, 2020.

Hudson, J. M. G. and Henry, G. H. R.: Increased plant biomass in a High Arctic heath community from 1981 to 2008, Ecology, 90, 2657-2663, https://doi.org/10.1890/09-0102.1, 2009.

IPCC: Annex II: Climate System Scenario Tables, in: Climate Change 2013: The Physical Science Basis. Contribution of Working Group I to the Fifth Assessment Report of the Intergovernmental Panel on Climate Change, edited by: Prather, M., Flato, G., Friedlingstein, P., Jones, C., Lamarque, J.-F., Liao, H., and Rasch, P., Cambridge University Press, Cambridge, United Kingdom and New York, NY, USA, 2013.

IPCC: Climate Change 2014: Synthesis Report. Contribution of Working Groups I, II and III to the Fifth Assessment Report of the Intergovernmental Panel on Climate Change [Core Writing Team, R.K. Pachauri and L.A. Meyer (eds.)]. Geneve, 151 pp.2014.

Johansson, T.: Biomass production and allometric above- and below-ground relations for young birch stands planted at four spacings on abandoned farmland, Forestry, 80, 41-52, https://doi.org/10.1093/forestry/cpl049, 2007.

Käyhkö, J. and Horstkotte, T.: Reindeer husbandry under global change in the tundra region of Northern Fennoscandia, Publications from the Department of Geography and Geology, University of Turku., 40, https://doi.org/https://doi.org/10.13140/RG.2.2.22151.39841, 2017.

Kosztra, B., Büttner, G., Hazeu, G., and Arnold, S.: Updated CLC illustrated nomenclature guidelines, European Topic Centre on Urban, land and soil systems, 126, 2019.

Kullman, L.: Ecological overview of past and recent history of the alpine tree line ecotone and plant cover in the Swedish Scandes (In Swedish with English summary), Svensk Botanisk Tidsskrift, 110, 132-272, 2016.

Kumpula, J., Kurkilahti, M., Helle, T., and Colpaert, A.: Both reindeer management and several other land use factors explain the reduction in ground lichens (Cladonia spp.) in pastures grazed by semi-domesticated reindeer in Finland, Regional Environmental Change, 14, 541-559, https://doi.org/10.1007/s10113-013-0508-5, 2014.

Kuuluvainen, T. and Gauthier, S.: Young and old forest in the boreal: critical stages of ecosystem dynamics and management under global change, Forest Ecosystems, 5, 26, https://doi.org/10.1186/s40663-018-0142-2, 2018.

Lagergren, F. and Miller, P. A.: LPJ-GUESS model results with arctic plant functional types (PFTs) for Fennoscandia from the BioDiv-Support project at RCP 8.5, DataGURU, https://doi.org/10.18161/j395-1j66, 2023.

856 Lagergren, F., Olin, S., and Miller, P. A.: Incorporating reindeer grazing and damage by ozone in LPJ-GUESS
857 for the BioDiv-Support project, Zenodo, https://doi.org/10.5281/zenodo.8262590, 2023.

858 Lamarque, J. F., Kyle, G. P., Meinshausen, M., Riahi, K., Smith, S. J., van Vuuren, D. P., Conley, A. J., and Vitt,
859 F.: Global and regional evolution of short-lived radiatively-active gases and aerosols in the Representative
860 Concentration Pathways, Climatic Change, 109, 191-212, https://doi.org/10.1007/s10584-011-0155-0, 2011.

861 Lamarque, J. F., Bond, T. C., Eyring, V., Granier, C., Heil, A., Klimont, Z., Lee, D., Liousse, C., Mieville, A.,
862 Owen, B., Schultz, M. G., Shindell, D., Smith, S. J., Stehfest, E., Van Aardenne, J., Cooper, O. R., Kainuma, M.,
863 Mahowald, N., McConnell, J. R., Naik, V., Riahi, K., and van Vuuren, D. P.: Historical (1850-2000) gridded
864 anthropogenic and biomass burning emissions of reactive gases and aerosols: methodology and application,
865 Atmospheric Chemistry and Physics, 10, 7017-7039, https://doi.org/10.5194/acp-10-7017-2010, 2010.

866 Lind, P., Belušić, D., Christensen, O. B., Dobler, A., Kjellström, E., Landgren, O., Lindstedt, D., Matte, D.,
867 Pedersen, R. A., Toivonen, E., and Wang, F. X.: Benefits and added value of convection-permitting climate
868 modeling over Fenno-Scandinavia, Climate Dynamics, 55, 1893-1912, https://doi.org/10.1007/s00382-020-
869 05359-3, 2020.

870 Lind, P., Pedersen, R. A., Kjellström, E., Landgren, O., Matte, D., Dobler, A., Belušić, D., Médus, E., Wang, F.,
871 Christensen, O. B., Christensen, J. H., and Verpe Dyrdal, A.: Climate change information over Fenno-Scandinavia
872 produced with a convection-permitting climate model, Climate Dynamics, In press,
873 https://doi.org/10.1007/s00382-022-06589-3, 2022.

874 Lindeskog, M., Smith, B., Lagergren, F., Sycheva, E., Ficko, A., Pretzsch, H., and Rammig, A.: Accounting for
875 forest management in the estimation of forest carbon balance using the dynamic vegetation model LPJ-GUESS
876 (v4.0, r9710): implementation and evaluation of simulations for Europe, Geoscientific Model Development, 14,
877 6071-6112, https://doi.org/10.5194/gmd-14-6071-2021, 2021.

878 Liu, Y., Riley, W. J., Keenan, T. F., Mekonnen, Z. A., Holm, J. A., Zhu, Q., and Torn, M. S.: Dispersal and fire
879 limit Arctic shrub expansion, Nature Communications, 13, 3843, https://doi.org/10.1038/s41467-022-31597-6,
880 2022.

881 Luoto, M. and Seppälä, M.: Thermokarst ponds as indicators of the former distribution of palsas in Finnish
882 lapland, Permafrost and Periglacial Processes, 14, 19-27, https://doi.org/10.1002/ppp.441, 2003.

883 Masson, V., Le Moigne, P., Martin, E., Faroux, S., Alias, A., Alkama, R., Belamari, S., Barbu, A., Boone, A.,
884 Bouyssel, F., Brousseau, P., Brun, E., Calvet, J.-C., Carrer, D., Decharme, B., Delire, C., Donier, S., Essaouini,
885 K., Gibelin, A.-L., Giordani, H., Habets, F., Jidane, M., Kerdraon, G., Kourzeneva, E., Lafaysse, M., Lafont, S.,
886 Brossier, C. L., Lemonsu, A., Mahfouf, J.-F., Marguinaud, P., Mokhtari, M., Morin, S., Pigeon, G., Salgado, R.,
887 Seity, Y., Taillefer, F., Tanguy, G., Tulet, P., Vincendon, B., Vionnet, V., and Voldoire, A.: The SURFEXv7.2
888 land and ocean surface platform for coupled or offline simulation of earth surface variables and fluxes,
889 Geoscientific Model Development, 6, 929-960, https://doi.org/10.5194/gmd-6-929-2013, 2013.

890 McEwan, E. H. and Whitehead, P. E.: Seasonal changes in the energy and nitrogen intake in reindeer and caribou,
891 Canadian Journal of Zoology, 48, 905-913, https://doi.org/10.1139/z70-164, 1970.

892 Mee, J. A. and Moore, J.-S.: The ecological and evolutionary implications of microrefugia, Journal of
893 Biogeography, 41, 837-841, https://doi.org/10.1111/jbi.12254, 2014.

894 Meinshausen, M., Smith, S. J., Calvin, K., Daniel, J. S., Kainuma, M. L. T., Lamarque, J. F., Matsumoto, K.,
895 Montzka, S. A., Raper, S. C. B., Riahi, K., Thomson, A., Velders, G. J. M., and van Vuuren, D. P. P.: The RCP
896 greenhouse gas concentrations and their extensions from 1765 to 2300, Climatic Change, 109, 213-241,
897 https://doi.org/10.1007/s10584-011-0156-z, 2011.

898 Miller, P. A. and Smith, B.: Modelling Tundra Vegetation Response to Recent Arctic Warming, Ambio, 41, 281-
899 291, https://doi.org/10.1007/s13280-012-0306-1, 2012.

900 Myers-Smith, I. H., Forbes, B. C., Wilmking, M., Hallinger, M., Lantz, T., Blok, D., Tape, K. D., Macias-Fauria,
901 M., Sass-Klaassen, U., Lévesque, E., Boudreau, S., Ropars, P., Hermanutz, L., Trant, A., Siegwart Collier, L.,
902 Weijers, S., Rozema, J., Rayback, S. A., Schmidt, N. M., Schaepman-Strub, G., Wipf, S., Rixen, C., Ménard, C.
903 B., Venn, S., Goetz, S., Andreu-Hayles, L., Elmendorf, S., Ravolainen, V., Welker, J., Grogan, P., Epstein, H. E.,
904 and Hik, D. S.: Shrub expansion in tundra ecosystems: dynamics, impacts and research priorities, Environmental
905 Research Letters, 6, 045509, https://doi.org/10.1088/1748-9326/6/4/045509, 2011.

906 Oksanen, L. and Virtanen, R.: Topographic, altitudinal and regional patterns in continental and suboceanic heath
907 vegetation of northern Fennoscandia, Acta Botanica Fennica, 153, 1-80, 1995.

908 Olofsson, J., Kitti, H., Rautiainen, P., Stark, S., and Oksanen, L.: Effects of summer grazing by reindeer on
909 composition of vegetation, productivity and nitrogen cycling, Ecography, 24, 13-24,
910 https://doi.org/10.1034/j.1600-0587.2001.240103.x, 2001.

911 Olofsson, J., Oksanen, L., Callaghan, T., Hulme, P. E., Oksanen, T., and Suominen, O.: Herbivores inhibit climate-
912 driven shrub expansion on the tundra, Global Change Biology, 15, 2681-2693, https://doi.org/10.1111/j.1365-
913 2486.2009.01935.x, 2009.

914 Olvmo, M., Holmer, B., Thorsson, S., Reese, H., and Lindberg, F.: Sub-arctic palsa degradation and the role of
915 climatic drivers in the largest coherent palsa mire complex in Sweden (Vissatvuopmi), 1955-2016, Scientific
916 Reports, 10, 8937, https://doi.org/10.1038/s41598-020-65719-1, 2020.

917 Ono, J., Watanabe, M., Komuro, Y., Tatebe, H., and Abe, M.: Enhanced Arctic warming amplification revealed
918 in a low-emission scenario, Communications Earth & Environment, 3, 27, https://doi.org/10.1038/s43247-022-
919 00354-4, 2022.

920 Osuch, M., Lawrence, D., Meresa, H. K., Napiorkowski, J. J., and Romanowicz, R. J.: Projected changes in flood
921 indices in selected catchments in Poland in the 21st century, Stochastic Environmental Research and Risk
922 Assessment, 31, 2435-2457, https://doi.org/10.1007/s00477-016-1296-5, 2017.

923 Pauli, H. and Halloy, S. R. P.: High Mountain Ecosystems Under Climate Change, in: Oxford Research
924 Encyclopedia of Climate Science, edited by: Pauli, H., and Halloy, S. R. P., Oxford University Press, 1-56,
925 https://doi.org/10.1093/acrefore/9780190228620.013.764, 2019.

926 Pearson, R. G., Phillips, S. J., Loranty, M. M., Beck, P. S. A., Damoulas, T., Knight, S. J., and Goetz, S. J.: Shifts
927 in Arctic vegetation and associated feedbacks under climate change, Nature Climate Change, 3, 673-677,
928 https://doi.org/10.1038/nclimate1858, 2013.

929 Porada, P., Ekici, A., and Beer, C.: Effects of bryophyte and lichen cover on permafrost soil temperature at large
930 scale, Cryosphere, 10, 2291-2315, https://doi.org/10.5194/tc-10-2291-2016, 2016.

931 Rantanen, M., Karpechko, A. Y., Lipponen, A., Nordling, K., Hyvärinen, O., Ruosteenoja, K., Vihma, T., and
932 Laaksonen, A.: The Arctic has warmed nearly four times faster than the globe since 1979, Communications Earth
933 & Environment, 3, 168, https://doi.org/10.1038/s43247-022-00498-3, 2022.

934 Rasmus, S., Horstkotte, T., Turunen, M., Landauer, M., Löf, A., Lehtonen, I., Rosqvist, G., and Holand, Ø.:
935 Reindeer husbandry and climate change - Challenges for adaptation, in: Reindeer Husbandry and Global
936 Environmental Change - Pastoralism in Fennoscandia, edited by: Horstkotte, T., Holand, Ø., Kumpula, J., and
937 Moen, J., Routledge, London, 99-117, https://doi.org/10.4324/9781003118565-8, 2022.

938 Robertson, L., Langner, J., and Engardt, M.: An Eulerian limited-area atmospheric transport model, Journal of
939 Applied Meteorology, 38, 190-210, https://doi.org/10.1175/1520-0450(1999)038<0190:Aelaat>2.0.Co;2, 1999.

940 Rosqvist, G. C., Inga, N., and Eriksson, P.: Impacts of climate warming on reindeer herding require new land-use
941 strategies, Ambio, 51, 1247–1262, https://doi.org/10.1007/s13280-021-01655-2, 2021.

942 Rundqvist, S., Hedenås, H., Sandström, A., Emanuelsson, U., Eriksson, H., Jonasson, C., and Callaghan, T. V.:
943 Tree and Shrub Expansion Over the Past 34 Years at the Tree-Line Near Abisko, Sweden, Ambio, 40, 683-692,
944 https://doi.org/10.1007/s13280-011-0174-0, 2011.

945 Sandström, P., Cory, N., Svensson, J., Hedenås, H., Jougda, L., and Borchert, N.: On the decline of ground lichen
946 forests in the Swedish boreal landscape: Implications for reindeer husbandry and sustainable forest management,
947 Ambio, 45, 415-429, https://doi.org/10.1007/s13280-015-0759-0, 2016.

948 Scharn, R., Little, C. J., Bacon, C. D., Alatalo, J. M., Antonelli, A., Björkman, M. P., Molau, U., Nilsson, R. H.,
949 and Björk, R. G.: Decreased soil moisture due to warming drives phylogenetic diversity and community transitions
950 in the tundra, Environmental Research Letters, 16, 064031, https://doi.org/10.1088/1748-9326/abfe8a, 2021.

951 Scharn, R., Brachmann, C. G., Patchett, A., Reese, H., Bjorkman, A. D., Alatalo, J. M., Björk, R. G., Jägerbrand,
952 A. K., Molau, U., and Björkman, M. P.: Vegetation responses to 26 years of warming at Latnjajaure Field Station,
953 northern Sweden, Arctic Science, 8, 858-877, https://doi.org/10.1139/as-2020-0042, 2022.

954 Shannon, C. E.: A mathematical theory of communication, The Bell System Technical Journal, 27, 379–423,
955 1948.

956 Smith, B., Prentice, I. C., and Sykes, M. T.: Representation of vegetation dynamics in the modelling of terrestrial
957 ecosystems: comparing two contrasting approaches within European climate space, Global Ecology and
958 Biogeography, 10, 621-637, https://doi.org/10.1046/j.1466-822X.2001.t01-1-00256.x, 2001.

959 Smith, B., Wårlind, D., Arneth, A., Hickler, T., Leadley, P., Siltberg, J., and Zaehle, S.: Implications of
960 incorporating N cycling and N limitations on primary production in an individual-based dynamic vegetation
961 model, Biogeosciences, 11, 2027-2054, https://doi.org/10.5194/bg-11-2027-2014, 2014.

962 Speed, J. D. M., Austrheim, G., Kolstad, A. L., and Solberg, E. J.: Long-term changes in northern large-herbivore
963 communities reveal differential rewilding rates in space and time, Plos One, 14,
964 https://doi.org/10.1371/journal.pone.0217166, 2019.

965 Stoessel, M., Moen, J., and Lindborg, R.: Mapping cumulative pressures on the grazing lands of northern
966 Fennoscandia, Scientific reports, 12, 16044-16044, https://doi.org/10.1038/s41598-022-20095-w, 2022.

967 Sturm, M., Racine, C., and Tape, K.: Climate change - Increasing shrub abundance in the Arctic, Nature, 411,
968 546-547, https://doi.org/10.1038/35079180, 2001.

969 Sundqvist, M. K., Moen, J., Björk, R. G., Vowles, T., Kytöviita, M.-M., Parsons, M. A., and Olofsson, J.:
970 Experimental evidence of the long-term effects of reindeer on Arctic vegetation greenness and species richness at
971 a larger landscape scale, Journal of Ecology, 107, 2724-2736, https://doi.org/10.1111/1365-2745.13201, 2019.

972 Tang, J., Miller, P. A., Persson, A., Olefeldt, D., Pilesjö, P., Heliasz, M., Jackowicz-Korczynski, M., Yang, Z.,
973 Smith, B., Callaghan, T. V., and Christensen, T. R.: Carbon budget estimation of a subarctic catchment using a
974 dynamic ecosystem model at high spatial resolution, Biogeosciences, 12, 2791-2808, https://doi.org/10.5194/bg-
975 12-2791-2015, 2015.

976 Thomas, S. C. and Martin, A. R.: Carbon Content of Tree Tissues: A Synthesis, Forests, 3, 332-352,
977 https://doi.org/10.3390/f3020332, 2012.

978 Venäläinen, A., Lehtonen, I., Laapas, M., Ruosteenoja, K., Tikkanen, O.-P., Viiri, H., Ikonen, V.-P., and Peltola,
979 H.: Climate change induces multiple risks to boreal forests and forestry in Finland: A literature review, Global
980 Change Biology, 26, 4178-4196, https://doi.org/10.1111/gcb.15183, 2020.

981 Vowles, T., Gunnarsson, B., Molau, U., Hickler, T., Klemedtsson, L., and Björk, R. G.: Expansion of deciduous
982 tall shrubs but not evergreen dwarf shrubs inhibited by reindeer in Scandes mountain range, Journal of Ecology,
983 105, 1547-1561, https://doi.org/10.1111/1365-2745.12753, 2017.

984 Vuorinen, K. E. M., Oksanen, L., Oksanen, T., Pyykönen, A., Olofsson, J., and Virtanen, R.: Open tundra persist,
985 but arctic features decline-Vegetation changes in the warming Fennoscandian tundra, Global Change Biology, 23,
986 3794-3807, https://doi.org/10.1111/gcb.13710, 2017.

987   Wania, R., Ross, I., and Prentice, I. C.: Integrating peatlands and permafrost into a dynamic global vegetation

988   model: 2. Evaluation and sensitivity of vegetation and carbon cycle processes, Global Biogeochemical Cycles,

989   23, GB3015, https://doi.org/10.1029/2008gb003413, 2009a.

990   Wania, R., Ross, I., and Prentice, I. C.: Integrating peatlands and permafrost into a dynamic global vegetation

991   model: 1. Evaluation and sensitivity of physical land surface processes, Global Biogeochemical Cycles, 23,

992   GB3014, https://doi.org/10.1029/2008gb003412, 2009b.

993   Wolf, A., Callaghan, T. V., and Larson, K.: Future changes in vegetation and ecosystem function of the Barents

994   Region, Climatic Change, 87, 51-73, https://doi.org/10.1007/s10584-007-9342-4, 2008.

995   Xu, J., Morris, P. J., Liu, J., and Holden, J.: PEATMAP: Refining estimates of global peatland distribution based

996   on a meta-analysis, Catena, 160, 134-140, https://doi.org/10.1016/j.catena.2017.09.010, 2018.

997   Yu, Q., Epstein, H., Engstrom, R., and Walker, D.: Circumpolar arctic tundra biomass and productivity dynamics

998   in response to projected climate change and herbivory, Global Change Biology, 23, 3895-3907,

999   https://doi.org/10.1111/gcb.13632, 2017.

1000   Zhang, W. X., Miller, P. A., Smith, B., Wania, R., Koenigk, T., and Döscher, R.: Tundra shrubification and tree-

1001   line advance amplify arctic climate warming: results from an individual-based dynamic vegetation model,

1002   Environmental Research Letters, 8, 034023, https://doi.org/10.1088/1748-9326/8/3/034023, 2013.

1003